

AD-A126 703

A MODEL OF THE TRAILING EDGE SEPARATION ON AN AIRFOIL

1/1

(U) VON KARMAN INST FOR FLUID DYNAMICS

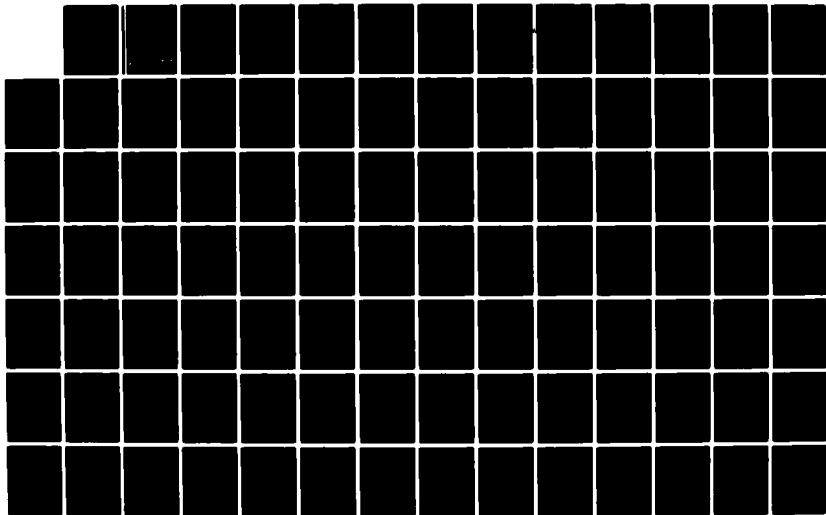
RHODE-SAINT-GENESE (BELGIUM) G ZILLIAC FEB 83

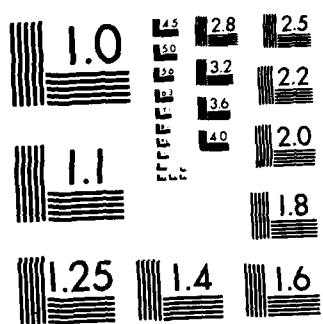
UNCLASSIFIED

EOARD-TR-83-7 AFOSR-82-0204

F/G 20/4

NL





MICROCOPY RESOLUTION TEST CHART
NATIONAL BUREAU OF STANDARDS-1963-A

ADA126703

BOARD-TR-83-7

GRANT AFOSR 82-0204

A MODEL OF THE TRAILING EDGE SEPARATION ON AN AIRFOIL

GREG ZILLIAC
VON KARMAN INSTITUTE FOR FLUID DYNAMICS
CHAUSSÉE DE WATERLOO, 72
B - 1640 RHODE SAINT GENÈSE, BELGIUM

FEBRUARY 1983

FINAL SCIENTIFIC REPORT, 15 MAY 1982 - 14 FEBRUARY 1983

APPROVED FOR PUBLIC RELEASE: DISTRIBUTION UNLIMITED

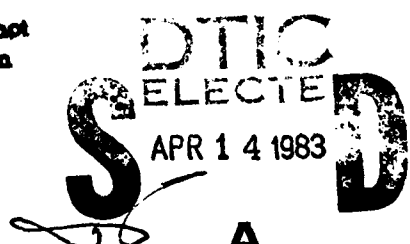
PREPARED FOR

Copy available to DTIC does not
permit fully legible reproduction

AIR FORCE OFFICE OF SCIENTIFIC RESEARCH
BOLLING AF BASE, DC 20332

AND

EUROPEAN OFFICE OF AEROSPACE RESEARCH AND DEVELOPMENT
LONDON, UK.



83 04 14 098

DISCLAIMER NOTICE

**THIS DOCUMENT IS BEST QUALITY
PRACTICABLE. THE COPY FURNISHED
TO DTIC CONTAINED A SIGNIFICANT
NUMBER OF PAGES WHICH DO NOT
REPRODUCE LEGIBLY.**

REPORT DOCUMENTATION PAGE		READ INSTRUCTIONS BEFORE COMPLETING FORM
1. REPORT NUMBER EOARD-TR-83-71	2. GOVT ACCESSION NO.	3. RECIPIENT'S CATALOG NUMBER
4. TITLE (and Subtitle) A MODEL OF THE TRAILING EDGE SEPARATION ON AN AIRFOIL		5. TYPE OF REPORT & PERIOD COVERED Final Scient. Rep. 15 May 82 - 14 Feb 83
		6. PERFORMING ORG. REPORT NUMBER
7. AUTHOR(s) Greg ZILLIAC		8. CONTRACT OR GRANT NUMBER(s) AFOSR 82-0204
9. PERFORMING ORGANIZATION NAME AND ADDRESS von Karman Institute for Fluid Dynamics, Chaussée de Waterloo, 72, B-1640 Rhode-Saint-Genèse, Belgium		10. PROGRAM ELEMENT, PROJECT, TASK AREA & WORK UNIT NUMBERS P.E. 61102F Proj/Task 2301/D1
11. CONTROLLING OFFICE NAME AND ADDRESS European Office of Aerospace R&D/CA Box 14 FPO New York 09510		12. REPORT DATE February 1983
		13. NUMBER OF PAGES 91
14. MONITORING AGENCY NAME & ADDRESS(if different from Controlling Office) European Office of Aerospace Research and Development/CA Box 14 FPO New York 09510		15. SECURITY CLASS. (of this report) UNCLASSIFIED
16. DISTRIBUTION STATEMENT (of this Report) Approved for public release; distribution unlimited		15a. DECLASSIFICATION/DOWNGRADING SCHEDULE
17. DISTRIBUTION STATEMENT (of the abstract entered in Block 20, if different from Report) Approved for public release; distribution unlimited.		
18. SUPPLEMENTARY NOTES		
19. KEY WORDS (Continue on reverse side if necessary and identify by block number) BOUNDARY LAYER SEPARATION; LIFT PREDICTION; TURBULENT BOUNDARY LAYER; TWO DIMENSIONAL FLOW; SEPARATED FLOW		
20. ABSTRACT (Continue on reverse side if necessary and identify by block number) A model of the turbulent boundary layer separation of a two dimensional airfoil has been investigated. The model consists of distributing sources on the contour in the separated region of sufficient strength to maintain the constant pressure characteristic of trailing edge boundary layer separation. A model for the attached boundary layer has also been included. An accurate estimation of maximum lift, pitching moment and pressure distribution have been obtained. A correct drag prediction has not been accomplished.		

EOARD - TR-83 E 7

This report has been reviewed by the EOARD Information Office and is releasable to the National Technical Information Service (NTIS). At NTIS it will be releasable to the general public, including foreign nations.

This technical report has been reviewed and is approved for publication.

Cary A. Fisher
CARY A FISHER

CARY A. FISHER
Colonel, USAF
Chief Scientist

Jerry Ray Botts

JERRY R. BETTIS
Lt Colonel, USAF
Deputy Commander

TABLE OF CONTENTS

ABSTRACT	ii
LIST OF SYMBOLS	iii
LIST OF FIGURES	v
1. INTRODUCTION	1
2. THEORETICAL FOUNDATION OF THE MODEL	3
2.1 The model	3
2.2 The inviscid and separated regimes	3
2.2.1 Governing equations	3
2.2.2 Numerical considerations	6
2.3 The boundary layer analysis	8
2.3.1 The integral boundary layer approach	8
2.3.2 The laminar boundary layer	10
2.3.3 Transition and separation	11
2.3.4 The turbulent boundary layer	12
2.4 The source distribution	13
2.5 Forces and moment on the airfoil	15
2.5.1 The pressure coefficient	15
2.5.2 Lift coefficient	16
2.5.3 Drag coefficient	16
2.5.4 Pitching moment coefficient	17
2.6 The computer program	18
3. RESULTS	19
4. CONCLUSIONS AND RECOMMENDATIONS	21
REFERENCES	22
APPENDIX A - DERIVATION AND SOLUTION OF THE INTEGRAL EQUATIONS	23
APPENDIX B - PROGRAM LISTINGS	31
FIGURES	71

ACKNOWLEDGEMENTS

There are many people who deserve recognition for their contributions to this work. The basic framework of the computer programs existed when I started to work on this project. These programs were written or modified mainly by S. Huo, and R.A. Van den Braembussche among others.

I would also like to give additional thanks to R.A. Van den Braembussche, who spend a lot of time helping me become familiar with the methods used.

Thanks also to Sharon Stanaway for her moral support and assistance in turning the lights off after long nights at the video terminal.

ABSTRACT

A model of the turbulent boundary layer separation of a two dimensional airfoil has been investigated. The model consists of distributing sources on the contour in the separated region of sufficient strength to maintain the constant pressure characteristic of trailing edge boundary layer separation. A model for the attached boundary layer has also been included. An accurate estimation of maximum lift, pitching moment and pressure distribution have been obtained. A correct drag prediction has not been accomplished.

LIST OF SYMBOLS

c_D	energy dissipation coefficient
c_f	skin friction coefficient
c	airfoil chord
f_x, f_y	singularity influence functions
m	exponent in Falkner-Skan velocity profile
r	transformed boundary layer variable
S	distance along contour non dimensionalized by chord
S^*	distance along contour in separated region
u_e	local external velocity
u_τ	skin friction velocity
v	local velocity on airfoil in the separated region
w_L	local velocity on airfoil
z	point on airfoil where velocity is calculated
$B(,)$	boundary layer function
$C'(,)$	boundary layer function
C_d	two dimensional drag coefficient
C_l	two dimensional lift coefficient
C_m	two dimensional pitching moment coefficient
C_p	pressure coefficient
$F()$	Falkner-Skan velocity profile function
G	function used in boundary layer analyses
H_{12}	momentum thickness form factor = δ^*/θ
H_{32}	energy thickness form factor = θ_H/θ
K	singularity influence matrix
L	Le Foll's form factor
p	pressure
Re_θ	Reynolds number based on the momentum thickness

TEPS,TESS	points just before airfoil trailing edge
U	component of the complex velocity in x-direction
V	component of the complex velocity in y-direction
W	complex velocity
X	Le Foll's Reynolds number
α	airfoil angle of attack or uniform stream basic flow vortex strength
β	uniform stream basic flow vortex strength
γ	total vortex strength
δ	outflow basic flow vortex strength
δ^*	boundary layer displacement thickness
ξ	point where singularity is located
η	Blasius variable
θ	boundary layer momentum thickness
θ_H	boundary layer energy thickness
λ	Le Foll's parameter for the velocity profile
μ	circulatory basic flow vortex strength
ν	kinematic viscosity
ξ, n	coordinate of the singularity point location
ρ_∞	freestream density
τ	shearing stress
ϕ	airfoil transformed coordinates
Γ	total circulation
π	pressure gradient

LIST OF FIGURES

- 1 The model
- 2 The airfoil coordinate system
- 3 Source distribution for the GA(W-1)
- 4 The basic computational procedure
- 5-14 Pressure coefficient for GA(W-1)
- 15 Lift coefficient for GA(W-1)
- 16 Pitching moment coefficient for GA(W-1)
- 17 Pressure coefficient for NACA 2412
- 18 Lift coefficient for NACA 2412

1. INTRODUCTION

Analytical solutions to the problem of boundary layer separation have long been sought after but few have been successful. The Navier-Stokes equations which govern flow separation have not been solved for high Reynolds number flows, hence existing analytical solutions must involve assumptions concerning the nature of separation. Empiricism and/or experimental results are often used. In these cases, the question arises as to whether we are obtaining solutions which accurately reflect the physics of the problem, or are we modeling a phenomenon. This paper deals with the latter of these possibilities.

One of the first and arguably the best analytical model of turbulent boundary layer separation was developed Jacob (Ref. 1). This model consists of using inviscid singularity methods to model a viscous phenomenon. Sources are distributed in the dead air region to maintain constant pressure (in this region). A constant pressure, dead air region is a characteristic of turbulent boundary layer separation on an airfoil. The boundary layer and outer inviscid region must simultaneously be accounted for to complete the picture. Jacob has used this model to achieve very accurate prediction of maximum lift.

A second model which has been used with similar success is the model proposed by Dvorak and Maskew (Ref. 2). Their model consists of placing vortices on the free shear layer. The strength of the vortices is such as to obtain constant pressure in the separated region.

There are many other methods which have a stronger physical basis, but surprisingly, do not give results which can compare with the quality of results of Jacob and Dvorak's techniques.

In this investigation, Jacob's model has been chosen, because it has been in existence longer and has proven its validity as a model.

It is the object of this investigation to develop the method to the point where an accurate estimation of the lift, drag, pitching moment and pressure distribution can be obtained for the turbulent boundary layer separation of a two dimensional airfoil.

The importance of this investigation is that a correct prediction of the maximum lift coefficient is required. An inaccurate estimation of $C_{l_{max}}$ can have drastic effects on the payload capacity of an aircraft (under estimation of $C_{l_{max}}$ by 0.1 can mean up to a 20% reduction in payload).

Two points must be emphasized before continuing. First, this method is only applicable as a design tool and will not give any insight into the mechanisms of separation. Secondly, separation is a three dimensional, and quite often unsteady phenomenon. This has been demonstrated by wind tunnel tests which have shown that under optimum conditions, it is difficult to obtain a truly two dimensional and steady measurement. Hence, the results of this research cannot directly be extended to a three dimensional situation.

2. THEORETICAL FOUNDATION OF THE MODEL

2.1 The model

The model is shown in figure 1. It consists of breaking down the separated flow over an airfoil into three regions :

Region 1 : the outer inviscid region which is modelled by line vortices placed on the contour of the airfoil;

Region 2 : the boundary layer characteristics which are determined by an integral boundary method (similar to Le Foll's method). The boundary layer effect is included by distributing sources to compensate for the displacement thickness.

Region 3 : the separated region is modelled by sources distributed on the contour of sufficient strength to maintain constant pressure on the airfoil in this region.

2.2 The inviscid and separated regimes

2.2.1 Governing equations

The governing equation for the model can be derived from the boundary contours. Three boundary conditions are required for the analysis. Application of these conditions gives a Glauert type integral expression for the velocity on the contour :

- (1) Uniform stream far upstream.
- (2) Normal velocity on the airfoil surface is zero (kinematic condition).
- (3) An equivalent Kutta condition.

In addition to the boundary conditions, an additional criterium that the pressure is constant in the separated region must be enforced. Conditions 1 & 2 give rise to the integral expression for the vortex strength in function of blade geometry, uniform velocity, and the source distribution.

$$U_{\infty} \frac{dy}{dS} - V_{\infty} \frac{dx}{dS} = \frac{1}{2\pi} \oint_Y(\zeta) \left[f_y(z, \zeta) \frac{dx}{dS} - f_x(z, \zeta) \frac{dy}{dS} \right] dS(\zeta) \\ + \frac{1}{2\pi} \oint_Q(z) \left[-f_x(z, \zeta) \frac{dx}{dS} + f_y(z, \zeta) \frac{dy}{dS} \right] dS(\zeta) \quad (2.1)$$

where:

$$f_y(z, \zeta) = \frac{(x-\xi)}{(x-\xi)^2 + (y-\eta)^2}$$

$$f_x(z, \zeta) = \frac{-(y-\eta)}{(x-\xi)^2 + (y-\eta)^2}$$

Martensen (Ref. 3) has shown that the flow over an airfoil may be considered as the superposition of four basic flows, a uniform stream in the x-direction, a uniform stream in the y-direction, a circulatory flow, and an outflow. Expression (2.1) becomes four integral expressions for the vortex strength of the basic flows.

Uniform stream in x-direction :

$$\frac{1}{2\pi} \oint_a(\zeta) \left[f_y(z, \zeta) \frac{dx}{dS} - f_x(z, \zeta) \frac{dy}{dS} \right] dS(\zeta) = \frac{dy}{dS} \quad (2.2)$$

Uniform stream in y-direction :

$$\frac{1}{2\pi} \oint_b(\zeta) \left[f_y(z, \zeta) \frac{dx}{dS} - f_x(z, \zeta) \frac{dx}{dS} \right] dS(\zeta) = \frac{dx}{dS} \quad (2.3)$$

Circulatory flow :

$$\frac{1}{2} \oint_c(\zeta) \left[f_y(z, \zeta) \frac{dx}{dS} - f_x(z, \zeta) \frac{dy}{dS} \right] dS(\zeta) = 0 \quad (2.4)$$

Outflow :

$$\begin{aligned} & \frac{1}{2\pi} \oint \delta(\theta) \left[f_y(z, \zeta) \frac{dx}{dS} - f_x(z, \zeta) \frac{dy}{dS} \right] dS(\zeta) \\ &= - \frac{1}{2\pi} \oint Q(\zeta) \left[f_x(z, \zeta) \frac{dx}{dS} - f_y(z, \zeta) \frac{dy}{dS} \right] dS(\zeta) \end{aligned} \quad (2.5)$$

Equation (2.1) has been split into one homogeneous and three non-homogeneous equations. The total solution is given by :

$$\gamma(\zeta) = U_\infty \gamma(\zeta) - V_\infty \beta(\zeta) + \Gamma \mu(\zeta) + \delta(\zeta) \quad (2.6)$$

The following supplementary equations are required because the circulatory basic flow is the only basic flow which contributes to the circulation (note Γ in equation 2.6) :

$$\oint \zeta(\zeta) dS(\zeta) = 0 \quad (2.7)$$

$$\oint \beta(\zeta) dS(\zeta) = 0 \quad (2.8)$$

$$\oint \mu(\zeta) dS(\zeta) = 1 \quad (2.9)$$

$$\oint \delta(\zeta) dS(\zeta) = 0 \quad (2.10)$$

Applying the equivalent Kutta condition determines the magnitude of the total circulation :

$$\gamma(TEPS) = - \gamma(TESS) \quad (2.11)$$

Solving for the circulation :

$$\Gamma = - \frac{U_\infty [\alpha(TEPS) + \alpha(TESS)] + V_\infty [\beta(TEPS) + \beta(TESS)] + [\delta(TEPS) + \delta(TESS)]}{[\mu(TEPS) + \mu(TESS)]}$$

The local velocity on the contour is given by :

$$w_L = \sqrt{r(\zeta)^2 + Q(\zeta)^2} \quad (2.13)$$

This expression contains a contribution due to the vortices and due to the sources (sources are distributed along the contour for the boundary layer model as well as the separation model).

It appears that the complexity of the problem has been increased by separating the flow into four basic flows and that is true. The major advantage of this approach is that the velocity on the contour for any angle of attack can be determined by substitution of the corresponding freestream velocity components in equation (2.6). One limitation is that if the source distributions is changed, the whole problem must be resolved.

The solution of these integral equations is not straightforward. The equations become singular when calculating the influence of a particular vortex (or source) at its origin. This difficulty can be avoided as shown in appendix A.

2.2.2 Numerical considerations

Attention must now be turned to the numerical side of the problem. The profile is placed in the x-y plane as shown in figure 2. A coordinate transformation is used :

$$x = \frac{c}{2} (1 - \cos\phi) \quad (2.14)$$

This transformation allows a greater number of singularities to be placed near the leading and trailing edges where the slope of the contour changes rapidly. The contour is divided into N segments of constant included angle $\Delta\phi$. On each segment, a line vortex of constant strength is placed. Line vortices have an advantage over point vortices in that a line vortex distribution more closely approximates the continuous vortex

distribution of the integral equations. The integral expressions are replaced by the following summations :

Uniform stream in x-direction :

$$\frac{1}{2\pi} \sum_{i=1}^N \alpha(\zeta_i) K(z_j, \zeta_i, \Delta\zeta_i) = \frac{dy_j}{dS} \quad (2.15)$$

Uniform stream in y-direction :

$$\frac{1}{2\pi} \sum_{i=1}^N \beta(\zeta_i) K(z_j, \zeta_i, \Delta\zeta_i) = \frac{dx_j}{dS} \quad (2.16)$$

Circulatory flow :

$$\frac{1}{2\pi} \sum_{i=1}^N \mu(\zeta_i) K(z_j, \zeta_i, \Delta\zeta_i) = 0 \quad (2.17)$$

Outflow :

$$\frac{1}{2\pi} \sum_{i=1}^N \delta(\zeta_i) K(z_j, \zeta_i, \Delta\zeta_i) = \frac{1}{2\pi} \frac{b}{a} Q(\zeta_i) K(z_j, \zeta_i, \Delta\zeta_i) \quad (2.18)$$

where the influence function K is given in appendix A.

The supplementary conditions become :

$$\sum_{i=1}^N \alpha(\zeta_i) \Delta S(\zeta_i) = 0 \quad (2.20)$$

$$\sum_{i=1}^N \beta(\zeta_i) \Delta S(\zeta_i) = 0 \quad (2.21)$$

$$\sum_{i=1}^N \mu(\zeta_i) \Delta S(\zeta_i) = 1 \quad (2.22)$$

$$\sum_{i=1}^N \delta(\zeta_i) \Delta S(\zeta_i) = 0 \quad (2.23)$$

Supposing that equations (2.15) through (2.19) must be satisfied in the points $j=1, N$ where the vortices are located and together with equations (2.20) through (2.23) one obtains a set of $4(N+1)$ equations with $4N$ unknowns. The unknowns are the vortex strength of the basic flows. However, a system of equations derived from an integral equation of the first kind is often ill-conditioned. This can be avoided if the kinetic condition is also applied at the intersection points of the line vortex. This leads to a set of $4(2N+1)$ equations with $4N$ unknowns, which can be treated by a least square technique. See Appendix A for further details.

2.3 The boundary layer analysis

2.3.1 The integral boundary layer approach

The method used for the boundary layer region is by S. Huo (Ref. 4) and is similar to Le Foll's method. Huo's method is based on two assumptions :

- (1) Local boundary layer velocity profile similarity.
- (2) The velocity profile is assumed to be a one parameter profile.

The integral boundary layer equations are :

Momentum :

$$d(\theta u_e^2) + \delta^* u_e du_e = c_f \frac{u_e^2}{2} ds \quad (2.24)$$

Energy :

$$d\left(\theta_H \frac{u_e^3}{2}\right) = c_D u_e^3 ds \quad (2.25)$$

where the skin friction coefficient is :

$$c_f = \frac{2\tau_w}{\rho u_e^2} \quad (2.26)$$

and the energy dissipation coefficient is :

$$c_D = \frac{2}{\rho u_\infty^3} \int_0^\infty \tau(y) \frac{\partial u}{\partial y} dy \quad (2.27)$$

The unknowns in equations (2.24) and (2.25) are δ^* , θ , θ_H , c_f and c_D . There are two equations at hand with five unknowns. In order to solve these equations, the following information is necessary :

- (1) A velocity profile law in the boundary layer.
- (2) A skin friction law.
- (3) A relation for the dissipation coefficient.

The velocity profile law will enable the determination of the relation between the shape factors H_{12} and H_{32} . Therefore, knowing two of the characteristic thicknesses of the boundary layer from equations (2.24) and (2.25) will allow the calculation of the other thicknesses. The skin friction and dissipation coefficients will be determined from the skin friction law and dissipation relation respectively. Hence, the complete boundary layer characteristics can be computed.

Le Foll bases his method on the idea that the boundary layer can be described in terms of a form factor and a characteristic length instead of the velocity and length. The main advantage of this approach is that the inverse procedure of specifying boundary layer characteristics and their solving for the corresponding velocity distribution is easily achieved. The inverse problem is not of interest in this investigation, but the method is rapidly applicable to the direct problem.

The parameters L (Truckenbrodt's parameter) and X are used by Le Foll to specify the boundary layer characteristics:

$$dL = \frac{1}{(H_{12}-1)} \frac{dH_{32}}{H_{32}} \quad X = \ln Re_{\theta H} + 2L \quad (2.28)$$

As they are directly related to each other, L and X can, therefore, replace H_{12} and Re_{θ} to characterize a boundary layer.

2.3.2 The laminar boundary layer

The assumed velocity profile is the Faulkner-Skan profile :

$$\frac{u}{u_e} = F(n, m) \quad n = y \sqrt{\frac{u_e}{S}} \quad u_e = S^m \quad (2.29)$$

Stewartson's transformation has been used with the Faulkner-Skan profile to extend the boundary layer calculation into the compressible regime.

The compressibility aspect of boundary layer separation is not included in the separation model, but it was felt that since a compressible boundary layer method was available and programmed), compressibility should be (and was) included in the boundary layer model.

The skin friction and dissipation relation are functions of the assumed velocity profile. For the laminar boundary layer :

$$c_f = - \frac{4a_2(m)}{\sqrt{Re_x}} \quad c_D = \frac{F_1(m)}{\sqrt{Re_x}} \quad (2.30)$$

To simplify the calculation, another change of variable is introduced :

$$r = \frac{Re_{\theta} H e^{2L}}{Re_{ref}} \quad (2.31)$$

The momentum and energy integral equations become :

$$dr = u_e C(L, r) dS = \frac{u_e C'(L)}{r Re_{ref}} dS \quad (2.32)$$

$$\frac{dL}{dS} = \frac{1}{u_e} \frac{du_e}{dS} - B(L, r) \frac{1}{r} \frac{dr}{dS} \quad (2.33)$$

The function $C'(L, r)$ and $B(L, r)$ are given in reference 5.

Equations (2.32) and (2.33) are two first order differential equations which are solved by a fourth order Runge-Kutta procedure.

2.3.3 Transition_and_separation

Transition from laminar to turbulent flow can occur if the boundary layer becomes unstable (dictated by Schlichting's stability curve). The unstable region is :

$$L + 0.011 - 0.005 X < 0 \quad (2.34)$$

Whether transition will actually occur depends on the turbulence level, pressure gradient, and Re_{θ} . A transition criterium has been developed by B. Roberts (Ref. 6) based on the experimental results of P.S. Granville. This criteria predicts transition if ΔRe_0 (the difference in Reynolds number between point of instability and point of transition) is larger than a specified amount (see Ref. 6).

The boundary layer may separate (laminar separation) before transition. Zero wall shear stress is used as the separation criteria. In the calculation of L, the integration constant is chosen so that L equals zero at separation. This corresponds to :

$$H_{12} = 4.03 \quad H_{32} = 1.515$$

Since the inviscid model makes no allowances for laminar separation regions, some approximations must be introduced. In all cases laminar separation bubbles followed by turbulent reattachment is suspected, the length of the bubble is neglected and a turbulent boundary layer is assumed from the point of laminar separation.

2.3.4 The turbulent boundary layer

The assumed velocity profile is a modified Falkner-Skan profile :

$$\frac{u}{u_e} = 1 - \frac{u_\tau}{u_e} \frac{g(n, 2)}{K} \quad (2.35)$$

The function $g(n, Z)$ in equation (2.35) is determined from a combination of experimental results and theory (see Ref. 5 for further details). The turbulent boundary layer is also applicable to compressible flow by the inclusion of Van Driest's generalized velocity.

The skin friction coefficient is determined from :

$$\frac{u_\tau}{u_e} = \frac{K}{\lambda - .5 - \ln \left(\frac{2/3 + \lambda/2}{K} \right) + KC + \ln Re_\delta^*} \quad (2.36)$$

The momentum and energy integral equations may be combined to obtain :

$$c_D = f(\delta, \theta, \theta_H) c_f \quad (2.37)$$

If or a given Mach number, similar solutions exist, a relation between the pressure gradient and velocity profile parameter G must also exist. Assume that :

$$\pi = \left(\frac{G+1.635}{6.1} \right)^2 - 1.8 \quad (2.38)$$

where :

$$\pi = \frac{\delta_i^*}{\tau_w} \frac{dp}{ds}$$

and :

$$G = \frac{u_e}{u_\tau} \left(1 - \frac{1}{H_{12i}} \right)$$

with these assumptions, sufficient information is available to solve the turbulent boundary layer characteristics. See reference 5 for further details.

Turbulent boundary layer separation is also indicated when L equals 0. At this point, the boundary layer calculation is stopped.

2.4 The source distribution

A source distribution is required for the separation region model. This distribution must be chosen in such a way as to maintain constant pressure (constant resultant velocity) in the separation region. Equation (2.1) which is in effect an expression for the resultant velocity on the airfoil indicates

that the source distribution should be a function of :

- (1) profile geometry;
- (2) upstream condition;
- (3) angle of attack;
- (4) separation point location;
- (5) velocity distribution.

This is a paradoxical situation. The source distribution depends on the velocity on the contour which in turn depends on the source distribution. Also, for a given airfoil, the fundamental relationship for the source distribution must be general enough to allow for changes in angle of attack. To change the source function for different angles of attack would defeat the purpose of using a functional relationship.

Figure 3 shows a typical source distribution used in this study. The functional relationship is :

$$Q = 2.5S^*V_{sep.} \sin\alpha \quad 0 \leq S^* \leq 0.4$$

$$Q = V_{sep.} \sin\alpha$$

$$Q = V_{sep.} \sin\alpha - (V_{sep.} \sin\alpha - 0.2)(5S^* - 3)^2 / 4$$

where :

S^* is the distance along the contour in the separated region

$V_{sep.}$ is the velocity in the separated region

This relationship is dependent on angle of attack, velocity in the separated point and location of separation point. It does not include influence of the velocity distribution (over the remainder of the airfoil) on the separated region or influence of the profile geometry. A function which includes all of these aspects was too difficult to determine.

A completely different approach to the problem, which avoids functional source distributions altogether was attempted. This involves an iterative procedure to find a source distribution maintained constant velocity in the separated region, but this procedure failed to converge.

Another possible approach would be to a priori specify the velocity in the separated region, and then analytically solve the inverse problem to find the source strength. There have been recent research efforts at VKI to model wing tunnel wall interference effects using source distributions determined by an inverse procedure. This research has shown that a solution of a nearly singular system of equations is necessary to find the appropriate source distribution. This sheds a little light on the question why the iterative processes failed.

In the unseparated region a source distribution for the boundary layer model is determined from :

$$Q = \frac{d}{ds} (u_e \delta^*) \quad (2.40)$$

This relationship determines the source strength required to compensate for the displacement thickness. This approach (the blowing approach) is considered easier to use than the alternative approach of using a displacement surface for a couple of reasons : the profile geometry does not have to be recalculated. The blowing approach is also more compatible with the separated flow model.

2.5 Forces and moment on the airfoil

2.5.1 The pressure coefficient

The pressure coefficient is computed from the classical relationship :

$$c_p = 1 - \frac{w^2}{u_\infty^2} \quad (2.41)$$

where :

$$c_p = \frac{p - p_\infty}{q_\infty} \quad q_\infty = \frac{1}{2} \rho u_\infty^2 \quad (2.42)$$

These expressions are a result of Bernoulli's equation and are valid because this is an inviscid model. It is assumed that the pressure on the airfoil is the same as the pressure along the free streamline. Also, no wake effects have been included.

2.5.2 Lift_coefficient

The lift coefficient can be computed directly from the Kutta Joukowski law :

$$\Gamma = \oint \gamma ds$$

$$L = \Gamma \rho u_\infty \quad (2.43)$$

$$c_L = 2 \Gamma$$

2.5.3 Drag_coefficient

An accurate determination of the drag for an airfoil with turbulent boundary layer separation is very difficult due to the following :

- (1) Integral boundary layer methods often do not predict the separation point exactly because these methods are not valid close to the separation points.
- (2) Singularity methods are not accurate near the airfoil trailing edge.
- (3) Surface roughness and freestream turbulence have a large influence.

(4) Wake effects have an effect especially when there is separation.

(5) The equivalent Kutta condition does not model the physical situation exactly.

(6) Deviations from constant pressure in the separated region can have a significant effect.

With these considerations in mind, the total drag is composed of a pressure contribution due to incomplete pressure recovery, and a viscous contribution due to the viscous shearing stresses. The viscous drag is :

$$c_{d_v} = \frac{D_v}{\frac{1}{2} \rho u_\infty^2 c} = \cos\alpha \int_0^{2\pi} c_f(\phi) \frac{dx}{d\phi} \left(\frac{w_L}{u_\infty} \right)^2 d\phi \\ + \sin\alpha \int_0^{2\pi} c_f(\phi) \frac{dy}{d\phi} \left(\frac{w_L}{u_\infty} \right)^2 d\phi \quad (2.44)$$

The pressure drag is :

$$c_{d_p} = \frac{D_p}{\frac{1}{2} \rho u_\infty^2 c} = - \cos\alpha \int_0^{2\pi} c_p(\phi) \frac{dy}{d\phi} d\phi \\ + \sin\alpha \int_0^{2\pi} c_p(\phi) \frac{dx}{d\phi} d\phi \quad (2.45)$$

The contribution of the separated region to the viscous drag is zero (c_f is zero in this region).

2.5.4 Pitching moment coefficient

The pitching moment is the integral of the pressure distribution over the contour and is given by :

$$C_{m_{1/4c}} = \frac{M}{\frac{1}{2} \rho u_\infty^2 c^2} = - \int_0^{2\pi} C_p(0.25-X) \frac{dx}{d\phi} d\phi + \int_0^{2\pi} C_p(0.25-X) \frac{dx}{d\phi} d\phi \quad (2.46)$$

Expression (2.46) is the pitching moment coefficient about the quarter chord.

2.6 The computer program

Four computer programs have been written which perform the calculations described in the preceding sections. The basic computational procedure is outlined in figure 4 and listings of the program along with examples of the input and output are in Appendix B.

The calculations have been split into four programs to facilitate ease of use and also to allow modification of the results of each program if required. Duplication of computation is also avoided, for example, if for a given airfoil, the angle of attack is changed, the calculation may start with the second program (instead of the first program).

3. RESULTS

The separated turbulent boundary layer for the GA(W-1) and the NACA 2412 airfoil have been investigated. The results of these investigations are presented in figures 5 through 18.

For the GA(W-1) airfoil, figures 5 and 6 show the inviscid and viscous pressure coefficient for low angles of attack. Notice that the viscous calculated pressure coefficient agrees very well with the experimental results (Ref. 7) except near the leading edge where there is a short laminar separation bubble.

At angles of attack greater than four degrees, computational difficulties arose. The boundary layer program was originally written and calibrated for turbomachinery applications and in cases where the pressure peaks near the leading edge become too great, the boundary layer calculation failed. A second problem was a short laminar separation bubble which existed throughout the angle of attack range.

Figures 7-14 show the results of the calculation where the experimental separation point has been used. The boundary layer model has not been included. The source distribution used for the separation region has been optimized for an angle of attack of about 18 degrees, hence for other angles of attack, the pressure distribution is not as constant (in the separation region) as it is for 18 degrees.

Figures 15 and 16 show the lift and pitching moment coefficient versus angle of attack respectively. Agreement with the experimental results is quite good. There is a deviation of the computed pitching moment coefficient at the high angles of attack. This is due to the calculated pressure distribution which differs slightly from the experimental pressure distribution for the high angle of attack cases. Since the boundary layer program failed, a calculation of the drag was not achieved.

Figure 17 shows the results of a computed pressure distribution for NACA 2414 airfoil. A very flat pressure distribution was obtained for this angle of attack. The lift curve for this airfoil is presented in figure 18. To obtain results for the NACA 2412 which included a prediction of the separation point the computational procedure was again modified.

- (1) The extremely high pressure peak near the leading edge was lowered (first five percent of airfoil).
- (2) An estimated separation point was used.
- (3) The boundary layer program was then used to validate the estimated separation point location.

It was felt that lowering the pressure peak was justifiable because the boundary layer program predicted laminar separation in the first five per cent. A short laminar separation bubble would lower the pressure peak and since there is no laminar separation model, the peak was lowered by using engineering judgement. Figure 17 shows that a good prediction of $C_{\ell_{\max}}$ was obtained.

4. CONCLUSIONS AND RECOMMENDATIONS

The following can be concluded about the investigation :

- (1) The model appears to be a valid model for turbulent boundary layer separation.
- (2) Could improve the method of determining the source distribution for the separated region. The inverse problem is a possibility. It will be very difficult to define an iterative procedure to find the source strength because of convergence problems.
- (3) The boundary layer program should be extended so that it can handle airfoils with high pressure peaks and at high Reynolds number.
- (4) A laminar separation model should be included.
- (5) The lift, pitching moment, and pressure distribution have been accurately predicted for two airfoils.
- (6) The drag has not been predicted.
- (7) A wake model should be incorporated.
- (8) Extension of the computer model to compressible flow is worth considering.

REFERENCES

1. JACOB, K.: Berechnung der abgelösten inkompressiblen Strömung um Tragflügelprofile und Bestimmung des maximalen Auftriebs.
Zeitschrift für Flugwissenschaften,
Bd. 17, Heft 7, Juli 1969, pp 221-230.
2. DVORAK, F.A. & MASKEW, B.: Application of the AMI C_{ℓ}^{\max} prediction method to a number of airfoils. In: Advanced Technology Airfoil Research.
NASA CP 2045, Vol. 1, 1978.
3. MARTENSEN, E.: Berechnung der Druckverteilung an Gitter-Profilen in ebener Potentialströmung mit einer Fredholmschen Integralgleichung.
Archive for Rational Mech. and Analysis,
Vol. 3, No. 3, 1959, pp 235.
4. HUO, S.: Optimization based on the boundary layer concept for compressible decelerating flows.
Ph.D. Thesis, ULB, October 1973.
5. PAPAILIOU, K.: Blade optimization based on boundary layer concepts.
VKI CN 60, 1967.
6. ROBERTS, W.B.: A study of the effects of Reynolds number and laminar separation bubbles on the flow through axial compressor cascades.
Ph.D. Thesis, ULB, May 1973.
7. McGHEE, R.J. & BEASLEY, W.D.: Low speed aerodynamic characteristics of a 17-percent-thick airfoil section designed for general aviation applications.
NASA TN D-7428, 1973.

APPENDIX A - DERIVATION AND SOLUTION
OF THE INTEGRAL EQUATIONS

Derivation of the integral equations

This appendix contains a detailed derivation of integral equations. Attention is also given to the solution of these equations.

The complex velocity at point x, y induced by a vortex at ξ, η is :

$$\bar{W}(z) = u - iv = - \frac{i}{2\pi} \frac{\gamma(\rho)}{x + iy} \quad (A.1)$$

where :

$$X = x - \xi \quad \text{and} \quad Y = y - \eta$$

The complex velocity due to a distribution of vortices on a closed contour is :

$$\bar{W}(z) = - \frac{i}{2\pi} \oint \frac{\gamma(\zeta)}{x + iy} dS(\zeta) \quad (A.2)$$

separating the complex velocity into its components :

$$U(z) = - \frac{1}{2\pi} \oint \frac{Y\gamma(\zeta)}{X^2 + Y^2} dS(\zeta) \quad (A.3)$$

$$V(z) = \frac{1}{2\pi} \oint \frac{X\gamma(\zeta)}{X^2 + Y^2} dS(\zeta) \quad (A.4)$$

A uniform stream must be superimposed :

$$\bar{W}_\infty = U_\infty + iV_\infty \quad (A.4)$$

$$U(z) = U_{\infty} - \frac{1}{2\pi} \oint \frac{Y\gamma(\zeta)}{X^2+Y^2} dS(\zeta) \quad (A.6)$$

$$V(z) = V_{\infty} + \frac{1}{2\pi} \oint \frac{X\gamma(\zeta)}{X^2+Y^2} dS(\zeta) \quad (A.7)$$

Sources are placed on the contour for the boundary layer model.

$$W(z) = \frac{1}{2\pi} \frac{Q(\zeta)}{X+iY} \quad (A.8)$$

For sources distributed on a contour, the complex velocity is :

$$W(z) = \frac{1}{2\pi} \oint \frac{Q(\zeta)}{X+iY} dS(\zeta) \quad (A.9)$$

Superimposing the source distribution :

$$U(z) = U_{\infty} - \frac{1}{2\pi} \oint \frac{Y\gamma'(\zeta)}{X^2+Y^2} dS(\zeta) + \frac{1}{2\pi} \oint \frac{XQ(\zeta)}{X^2+Y^2} dS(\zeta) \quad (A.10)$$

$$V(z) = V_{\infty} + \frac{1}{2\pi} \oint \frac{Y\zeta}{X^2+Y^2} dS(\zeta) - \frac{1}{2\pi} \oint \frac{YQ(\zeta)}{X^2+Y^2} dS(\zeta) \quad (A.11)$$

The kinetic boundary condition that the velocity normal to the airfoil surface is zero is enforced. This is equivalent to stating that the surface is a streamline.

$$\frac{\partial \psi}{\partial S} = 0$$

$$\frac{\partial \psi}{\partial S} = \frac{\partial \psi}{\partial x} \frac{dx}{dS} + \frac{\partial \psi}{\partial y} \frac{dy}{dS}$$

$$0 = U(z) \frac{dy}{dS} - V(z) \frac{dx}{dS} \quad (\text{A.12})$$

Introducing (A.10) and (A.11) one obtains :

$$\begin{aligned} 0 = U_\infty \frac{dy}{dS} - & \left[\frac{1}{2\pi} \oint \frac{Y\gamma(\zeta)}{X^2+Y^2} dS(\zeta) \right] \frac{dy}{dS} \\ & + \left[\frac{1}{2\pi} \oint \frac{XQ(\zeta)}{X^2+Y^2} dS(\zeta) \right] \frac{dy}{dS} \quad (\text{A.13}) \\ - V_\infty \frac{dx}{dS} - & \left[\frac{1}{2\pi} \oint \frac{X\gamma(\zeta)}{X^2+Y^2} dS(\zeta) \right] \frac{dx}{dS} \\ & + \left[\frac{1}{2\pi} \oint \frac{YQ(\zeta)}{X^2+Y^2} dS(\zeta) \right] \frac{dx}{dS} \end{aligned}$$

Since $dS(\zeta)$ is not a function of x, y the derivatives $\frac{dy}{dS}$ and $\frac{dx}{dS}$ can be taken inside the integral.

$$\begin{aligned} U_\infty \frac{dy}{dS} - V_\infty \frac{dx}{dS} = & \frac{1}{2\pi} \oint \gamma(\zeta) \left[f_y(z, \zeta) \frac{dx}{dS} - f_x(z, \zeta) \frac{dy}{dS} \right] dS(\zeta) \\ & + \frac{1}{2\pi} \oint Q(\zeta) \left[f_x(z, \zeta) \frac{dx}{dS} - f_y(z, \zeta) \frac{dy}{dS} \right] dS(\zeta) \quad (\text{A.14}) \end{aligned}$$

where :

$$f_y(z, \zeta) = \frac{x}{X^2+Y^2} \qquad f_x(z, \zeta) = - \frac{y}{X^2+Y^2}$$

Integral expression (A.14) can be split into one homogeneous and three non-homogeneous equations corresponding to the four basic flows described in chapter 2.

$$\frac{1}{2\pi} \oint \alpha(\zeta) \left[f_y(z, \zeta) \frac{dx}{dS} - f_x(z, \zeta) \frac{dy}{dS} \right] dS(\zeta) = \frac{dy}{dS} \quad (A.15)$$

$$\frac{1}{2\pi} \oint \beta(\zeta) \left[f_y(z, \zeta) \frac{dx}{dS} - f_x(z, \zeta) \frac{dy}{dS} \right] dS(\zeta) = \frac{dx}{dS} \quad (A.16)$$

$$\frac{1}{2\pi} \oint \mu(\zeta) \left[f_y(z, \zeta) \frac{dx}{dS} - f_x(z, \zeta) \frac{dy}{dS} \right] dS = 0 \quad (A.17)$$

$$\begin{aligned} \frac{1}{2\pi} \oint \delta(\zeta) \left[f_y(z, \zeta) \frac{dx}{dS} - f_x(z, \zeta) \frac{dy}{dS} \right] dS(\zeta) \\ = - \frac{1}{2\pi} \oint Q(\zeta) \left[f_x(z, \zeta) \frac{dx}{dS} - f_y(z, \zeta) \frac{dy}{dS} \right] dS(\zeta) \end{aligned} \quad (A.18)$$

The total vortex strength is the superposition of the four basic vortex strengths.

$$\gamma(\zeta) = U_\infty \alpha(\zeta) - V_\infty \beta(\zeta) + \Gamma \mu(\zeta) + \delta(\zeta) \quad (A.19)$$

Equations (A.15) through (A.18) are obtained by substituting equation (A.19) into (A.14) and collecting like terms.

The far field boundary condition (uniform stream far upstream) has been implicitly satisfied. This can be demonstrated by taking the limit of (A.10) and (A.11). As x approaches infinity, the velocity components become equivalent to the imposed uniform stream. This result shows that the singularities do not have an influence far upstream.

The supplementary equations (as described in chapter 2) are :

$$\oint \alpha(\zeta) dS(\zeta) = 0 \quad (A.20)$$

$$\oint \beta(\zeta) dS(\zeta) = 0 \quad (A.21)$$

$$\oint \mu(\zeta) dS(\zeta) = 1 \quad (A.22)$$

$$\oint \delta(\zeta) dS(\zeta) = 0 \quad (A.23)$$

The equivalent Kutta condition fixes the circulation :

$$\gamma(TEPS) = -\gamma(TESS) \quad (A.24)$$

Using equations (A.19 and A.24) gives :

$$r = \frac{-U_\infty [\alpha(TEPS) + \alpha(TESS)] + V_\infty [\beta(TEPS) + \beta(TESS)] + [\delta(TEPS) + \delta(TESS)]}{[\mu(TEPS) + \mu(TESS)]} \quad (A.25)$$

Solution of the integral equations

The solution of the integral equations is complicated by the fact that expressions (A.15) through (A.18) are singular integrals. Before the discussion of the singular integrals, a coordinate transformation which allows greater numerical accuracy will be performed :

$$x = \frac{c}{2} (1 - \cos \phi) \quad (A.26)$$

Hence :

$$\frac{dy}{dS} = \frac{dy}{d\phi} \frac{d\phi}{dS} \quad \frac{dx}{dS} = \frac{dx}{d\phi} \frac{d\phi}{dS}$$

$$dS(z) = \sqrt{\left(\frac{\partial x}{\partial \phi}\right)^2 + \left(\frac{\partial y}{\partial \phi}\right)^2} d\phi(z) \quad (A.27)$$

Similarity :

$$dS(\xi) = \sqrt{\left(\frac{\partial \xi}{\partial \phi}\right)^2 + \left(\frac{\partial \eta}{\partial \phi}\right)^2} d\phi(\xi) \quad (A.28)$$

A new variable will be introduced :

$$\gamma'(\xi) = \gamma(\xi) \sqrt{\left(\frac{\partial \xi}{\partial \phi}\right)^2 + \left(\frac{\partial \eta}{\partial \phi}\right)^2} \quad (A.29)$$

This definition of the vortex strength has no physical significance, it is just used to simplify the derivation. This definition also applies to the basic flow vortex strengths.

The singular integral

Expressions (A.15) through (A.18) are singular integrals. This computational difficulty can be avoided by finding a function whose derivative is equal to the integral. Thus the integrals will become equivalent to the function evaluated between the limits of integration. The function $I(z, \xi)$ must be determined such that :

$$\frac{dI(z, \xi)}{d\phi(\xi)} = \left[f_y(z, \xi) \frac{dx}{d\phi} - f_x(z, \xi) \frac{dy}{d\phi} \right] \quad (A.30)$$

Make the following assumptions :

(1) $\gamma'(\xi)$ is constant over the distance $\phi - \frac{\Delta\phi}{2}$ to $\phi + \frac{\Delta\phi}{2}$ so that the vortex strength in (A.15) through (A.18) can be taken out from under the integral sign.

(2) Also assume that $\frac{\partial x}{\partial \phi}(\gamma)$ and $\frac{\partial y}{\partial \phi}(\xi)$ are constant in that region.

Define the following two functions :

$$F(z, \zeta) = \operatorname{atan} \frac{x}{y} \quad G(z, \zeta) = \frac{1}{2} \ln (x^2 + y^2)$$

Hence :

$$\frac{dG(z, \zeta)}{d\phi(\zeta)} = \frac{-x \frac{d\zeta}{d\phi(\zeta)} - y \frac{dy}{d\phi(\zeta)}}{x^2 + y^2}$$

$$\frac{dF(z, \zeta)}{d\phi(\zeta)} = \frac{x \frac{dx}{d\phi(\zeta)} - y \frac{d\zeta}{d\phi(\zeta)}}{x^2 + y^2}$$

Now multiply $\frac{dF}{d\phi(\zeta)}$ by C_1 and $\frac{dG}{d\phi(\zeta)}$ by C_2 where :

$$C_1 = \frac{\frac{d\zeta}{d\phi(\zeta)} \frac{dx}{d\phi(z)} - \frac{dx}{d\phi(z)} \frac{d\zeta}{d\phi(\zeta)}}{\left(\frac{d\zeta}{d\phi(\zeta)} \right)^2 + \left(\frac{dy}{d\phi(\zeta)} \right)^2}$$

$$C_2 = \frac{\frac{d\zeta}{d\phi(\zeta)} \frac{dx}{d\phi(z)} + \frac{dy}{d\phi(z)} \frac{d\zeta}{d\phi(\zeta)}}{\left(\frac{d\zeta}{d\phi(\zeta)} \right)^2 + \left(\frac{dy}{d\phi(\zeta)} \right)^2}$$

After simplification, it can be shown that the function $I(z, \zeta)$ in (A.30) has been obtained.

$$\frac{dI(z, \zeta)}{d\phi(\zeta)} = C_1 \frac{dF}{d\phi(\zeta)} + C_2 \frac{dG}{d\phi(\zeta)} \quad (\text{A.31})$$

$$I(z, \zeta) = C_1 F(z, \zeta) + C_2 G(z, \zeta) \quad (\text{A.32})$$

Hence the integral equations (A.15) through (A.18) reduce to the following summations :

$$\frac{1}{2\pi} \sum_{i=1}^N \alpha'(\zeta_i) K(z, \zeta_i, \Delta\zeta_i) = \frac{dy_j}{d\phi} \quad (A.33)$$

$$\frac{1}{2\pi} \sum_{i=1}^N \beta'(\zeta_i) K(z, \zeta_i, \Delta\zeta_i) = \frac{dx_j}{d\phi} \quad (A.34)$$

$$\frac{1}{2\pi} \sum_{i=1}^N \mu'(\zeta_i) K(z, \zeta_i, \Delta\zeta_i) = 0 \quad (A.35)$$

$$\frac{1}{2\pi} \sum_{i=1}^N \delta'(\zeta_i) K(z, \zeta_i, \Delta\zeta_i) \quad (A.36)$$

$$= - \frac{1}{2\pi} \oint Q'(\zeta) \left[f_x(z, \zeta) \frac{dx}{d\phi} - f_y \frac{dy}{d\phi} \right] dS(\zeta)$$

where :

$$K(z, \zeta_i, \Delta\zeta_i) = I \left(z, \zeta_i + \frac{\Delta\zeta_i}{2} \right) - I \left(z, \zeta_i - \frac{\Delta\zeta_i}{2} \right) \quad (A.37)$$

The supplementary conditions are :

$$\sum_{i=1}^N \alpha(\zeta_i) \Delta S(\zeta_i) = 0 \quad (A.38)$$

$$\sum_{i=1}^N \beta(\zeta_i) \Delta S(\zeta_i) = 0 \quad (A.39)$$

$$\sum_{i=1}^N \mu(\zeta_i) \Delta S(\zeta_i) = 1 \quad (A.40)$$

$$\sum_{i=1}^N \delta(\zeta_i) \Delta S(\zeta_i) = 0 \quad (A.41)$$

APPENDIX B - PROGRAM LISTINGS

Copy available to DTIC does not permit fully legible reproduction.

C TRANSLATE THE PROFILE COORDINATES.

```

IF(L1.GE.4) GO TO 19
16 = IABS(J6-4)
DO 16+1 K=1,16
  IF(NGC.EQ.0,2) GOTO 16
    AC(K)=VEC(K)
    FX(K)=YEC(K)
    FY(K)=-YEC(K)
    GU TO 17
  16 ACK=-S1(C)
    FX(K)=-X1(N)
    FY(K)=-Y1(N)
  17 N=N-1
    I6=I6+1
    GU TO 20
  19 IF(C1.GT.412) GU TO 25
    N=J6-5
  20 N=23 K=16,6
    IF(C1.EQ.0,2) GOTO 22
      ACK=SE(C)
      FX(K)=XEC(N)
      FY(K)=YEC(N)
      GU TO 23
    22 ACK=S1(N)
      FX(K)=X1(N)
      FY(K)=Y1(N)
    23 N=N+1
      GU TO 34
    25 N=13-N
      DO 26 K=1,16
        IF(NGC.EQ.0,2) GOTO 27
          ACK=SE(C)
          FX(K)=X1(N)
          FY(K)=Y1(N)
          GU TO 28
        27 ACK=S1(N)
          FX(K)=X1(N)
          FY(K)=Y1(N)
        28 N=N+1
        I6=I6+1
        GU TO 31
      26 DO 32 F=16,6
        IF(NGC.EQ.0,2) GOTO 31
          ACK=2.*S1(N)-S1(N)
          FX(K)=2.*X1(N)+2.*Y1(N)
          FY(K)=-YEC(N)
          GU TO 32
        31 ACK=2.*S1(N)-S1(N)
          FX(K)=X1(N)+2.*Y1(N)
          FY(K)=-Y1(N)
        32 N=N-1
        DO 33 F=1,4
          IF(NGC.EQ.0,2) GOTO 34
            ACK=S1(N)
            FX(K)=X1(N)
            FY(K)=Y1(N)
            CALL I11(N,AL,A,FY)
            YF(N)=FY(N)
          33 GU TO 34
        34 IF(S1(C).GT.S1(N)) GU TO 14
          CALL I11(N,AL,A,FY)
        35 J6=I6+1
      
```

C CALCULATE THE TRANSFORMED PROFILE COORDINATES.

```

CT=P/LOAT(RP)
CT=P/LOAT(RP)
PA=I*(J1-J1)*CT
CF=CG(C)
SF=SSE(C)
SS=SF*(1.-CF)/2.*SSE(SSI))
10 S1(J)=S1*(1.-R*CF)/2.
DO 41 NC=1,2
  N1=6*I-1
  N2=6*I-2
  N3=6*I+1
  DO 42 J=2,RP
    DO 43 I=1,N1
      IF(NGC.EQ.0,2) GOTO 12
      GU TO 13
      CALL I11(N1,AL,A,FY)
      X1(E(J))=FX(I)
      Y1(E(J))=FY(I)
      CALL I11(N1,AL,A,FY)
      YF(I)=FY(I)
    12 IF(S1(C).GT.S1(N)) GU TO 14
    13 CALL I11(N1,AL,A,FY)
    14 J6=I2+1
  
```


- 39 -

SFC. 4 FOR

TECHNIQUE 10:1) MURTE(2,103)

10

every year and does not permit fully legible reproduction.

C LARAH (SESSION CULCX)
 SUBROUTINE LARAH(X,Y,M1,X1,Y1)
 SUBROUTINE A(3),I(4),Y(4),X(4)
 DATA M1
 DATA I(4)
 1 DO 25 K=1,4P
 2 Y(1)=A(3)*X(1)-X(1)+Y(1)*(K+1)*(X1-X(K))/((X(I)-X(K))
 3 IF (I(1)-4,3,1)
 4 Y(1)=A(3)
 5 RETURN
 C** TYPE FFCT
 SUBROUTINE DERH(S,XX(S),YY(S),DE(S))
 SUBROUTINE DERH(S,XX(S),YY(S),A1(S),A2(S),A3(S),A2(3),S(1),M(1),DER(1))
 M(1)
 11 IF (1,0,1)=JU,5
 12 JU=1
 13 X(1)=S(L)
 14 YY(1)=X(L)
 15 V2=+1
 16 M=V2-L+5
 17 X(1)=X(M)
 18 YY(1)=Y(M)
 19 V2=+2,26,18
 20 G0=1,1,5E
 21 M=1,1,43
 22 X(1)=X(M)
 23 YY(1)=Y(M)
 24 G0=1,1,4E
 25 V2=+2,20,21,21
 26 M=1,1,4
 27 X(1)=X(M)
 28 YY(1)=Y(M)
 29 V2=+1,4
 30 M=1,1,3
 31 X(1)=X(M)
 32 G0=1,1,2
 33 M=1,1,1
 34 X(1)=X(M)
 35 YY(1)=Y(M)
 36 V2=+1,4
 37 M=1,1,1
 38 X(1)=X(M)
 39 YY(1)=Y(M)
 40 V2=+1,4
 41 M=1,1,1
 42 X(1)=X(M)
 43 YY(1)=Y(M)
 44 V2=+1,4
 45 M=1,1,1
 46 X(1)=X(M)
 47 YY(1)=Y(M)
 48 V2=+1,4
 49 M=1,1,1
 50 X(1)=X(M)
 51 YY(1)=Y(M)
 52 V2=+1,4
 53 M=1,1,1
 54 X(1)=X(M)
 55 YY(1)=Y(M)
 56 V2=+1,4
 57 M=1,1,1
 58 X(1)=X(M)
 59 YY(1)=Y(M)
 60 V2=+1,4
 61 M=1,1,1
 62 X(1)=X(M)
 63 YY(1)=Y(M)
 64 V2=+1,4
 65 M=1,1,1
 66 X(1)=X(M)
 67 YY(1)=Y(M)
 68 V2=+1,4
 69 M=1,1,1
 70 X(1)=X(M)
 71 YY(1)=Y(M)
 72 V2=+1,4
 73 M=1,1,1
 74 X(1)=X(M)
 75 YY(1)=Y(M)
 76 V2=+1,4
 77 M=1,1,1
 78 X(1)=X(M)
 79 YY(1)=Y(M)
 80 V2=+1,4
 81 M=1,1,1
 82 X(1)=X(M)
 83 YY(1)=Y(M)
 84 V2=+1,4
 85 M=1,1,1
 86 X(1)=X(M)
 87 YY(1)=Y(M)
 88 V2=+1,4
 89 M=1,1,1
 90 X(1)=X(M)
 91 YY(1)=Y(M)
 92 V2=+1,4
 93 M=1,1,1
 94 X(1)=X(M)
 95 YY(1)=Y(M)
 96 V2=+1,4
 97 M=1,1,1
 98 X(1)=X(M)
 99 YY(1)=Y(M)
 100 V2=+1,4
 101 M=1,1,1
 102 X(1)=X(M)
 103 YY(1)=Y(M)
 104 V2=+1,4
 105 M=1,1,1
 106 X(1)=X(M)
 107 YY(1)=Y(M)
 108 V2=+1,4
 109 M=1,1,1
 110 X(1)=X(M)
 111 YY(1)=Y(M)
 112 V2=+1,4
 113 M=1,1,1
 114 X(1)=X(M)
 115 YY(1)=Y(M)
 116 V2=+1,4
 117 M=1,1,1
 118 X(1)=X(M)
 119 YY(1)=Y(M)
 120 V2=+1,4
 121 M=1,1,1
 122 X(1)=X(M)
 123 YY(1)=Y(M)
 124 V2=+1,4
 125 M=1,1,1
 126 X(1)=X(M)
 127 YY(1)=Y(M)
 128 V2=+1,4
 129 M=1,1,1
 130 X(1)=X(M)
 131 YY(1)=Y(M)
 132 V2=+1,4
 133 M=1,1,1
 134 X(1)=X(M)
 135 YY(1)=Y(M)
 136 V2=+1,4
 137 M=1,1,1
 138 X(1)=X(M)
 139 YY(1)=Y(M)
 140 V2=+1,4
 141 M=1,1,1
 142 X(1)=X(M)
 143 YY(1)=Y(M)
 144 V2=+1,4
 145 M=1,1,1
 146 X(1)=X(M)
 147 YY(1)=Y(M)
 148 V2=+1,4
 149 M=1,1,1
 150 X(1)=X(M)
 151 YY(1)=Y(M)
 152 V2=+1,4
 153 M=1,1,1
 154 X(1)=X(M)
 155 YY(1)=Y(M)
 156 V2=+1,4
 157 M=1,1,1
 158 X(1)=X(M)
 159 YY(1)=Y(M)
 160 V2=+1,4
 161 M=1,1,1
 162 X(1)=X(M)
 163 YY(1)=Y(M)
 164 V2=+1,4
 165 M=1,1,1
 166 X(1)=X(M)
 167 YY(1)=Y(M)
 168 V2=+1,4
 169 M=1,1,1
 170 X(1)=X(M)
 171 YY(1)=Y(M)
 172 V2=+1,4
 173 M=1,1,1
 174 X(1)=X(M)
 175 YY(1)=Y(M)
 176 V2=+1,4
 177 M=1,1,1
 178 X(1)=X(M)
 179 YY(1)=Y(M)
 180 V2=+1,4
 181 M=1,1,1
 182 X(1)=X(M)
 183 YY(1)=Y(M)
 184 V2=+1,4
 185 M=1,1,1
 186 X(1)=X(M)
 187 YY(1)=Y(M)
 188 V2=+1,4
 189 M=1,1,1
 190 X(1)=X(M)
 191 YY(1)=Y(M)
 192 V2=+1,4
 193 M=1,1,1
 194 X(1)=X(M)
 195 YY(1)=Y(M)
 196 V2=+1,4
 197 M=1,1,1
 198 X(1)=X(M)
 199 YY(1)=Y(M)
 200 V2=+1,4
 201 M=1,1,1
 202 X(1)=X(M)
 203 YY(1)=Y(M)
 204 V2=+1,4
 205 M=1,1,1
 206 X(1)=X(M)
 207 YY(1)=Y(M)
 208 V2=+1,4
 209 M=1,1,1
 210 X(1)=X(M)
 211 YY(1)=Y(M)
 212 V2=+1,4
 213 M=1,1,1
 214 X(1)=X(M)
 215 YY(1)=Y(M)
 216 V2=+1,4
 217 M=1,1,1
 218 X(1)=X(M)
 219 YY(1)=Y(M)
 220 V2=+1,4
 221 M=1,1,1
 222 X(1)=X(M)
 223 YY(1)=Y(M)

```

442 H12=1.42/AL*0.15
      RETURN
      END
      C GMF SUBROUTINE GMF(GA,O,RMSI,RMS,RM,U)
      C SUBROUTINE USED TO COVER VARIOUS MACH NO. RM AND LAVAL NO. RMS
      C IF THE REFERENCE LAVAL NO. RMSI IS GIVEN
      C DATE 22. 1. 72
      C
      UEXP(CO)
      RMS=URMSI
      RMFF=URMS
      RETURN
      END
      C SUBROUTINE SF(ORM,RLA,FU,FV,CA,CB,KW,UDL,F)
      COMMACH,EFC,FDC,DUM(4),IPRINT,DUM(4),CDV(480)
      C SUBROUTINE FOR CALCULATION OF THE SKIN FRICTION FOR THE COMPRESSIBLE
      C FLOW UP TO MACH 3.73
      C MODIFICATION TO ACCFELATE CONVERGENCE 31. 7. 75.
      C
      CALL SUBLRA(FU,PRM,DEL)
      CR=(ALGCR*RM/DEL)+(RLA-0.5)/0.41+5.
      AL=0.
      F=1.
      CLE=CA*(F)-ALOG(F)/.41
      UC=CL/CA
      GC=CC/(CC-CL)*.30001
      AN=AN+.1
      IPR=IPR+1
      IF(IPR>10)7.7
      IF(IITER>10)7.2
      IF(IITER>10)7.1
      WRITE(2,8)ITER,CA,CR,F,CL,CR,DC
      CUR=ITER
      IITER=IITER+1
      6 CUR+1
      UC=CL/CA
      GC=CC/(CC-CL)*.41
      IF(CD>.001)1.1/2
      DFELF*(CA/(CA+1.))*2.)
      F=FF-UF
      9 IF(F<.9,.5
      F=.0001
      10 TC(.5
      1 CONTINUE
      RETURN
      END
      C SUBROUTINE SCFL(RLA,FU,PRM,DEL)
      C SUBROUTINE TO CALCULATE THE DISPLACEMENT THICKNESS FOR COMPRESSIBLE
      C TURBULENT BOUNDARY LAYER USING DEFELD'S PROFILE
      C
      DIMENSION U(50),ADFL(50),X(50)
      I=49
      RFL=FLD(1)
      DO 101 I=1,4
      RFL=LU(1)
      X((I*(K1-1))+1,(RN-1))
      DFL(49)=I=2,N
      101
      RETURN

```

Copy available to DTIC does not
permit fully legible reproduction

```

C FT FUNCTION FT(GA, RM)
49 C FUNCTION USED TO CALCULATE THE RATIO OF TACTIAL TEMPERATURE TO STATIC
C TEMPERATURE WHEN THE MACH NO. RM IS GIVEN.
C FT=1+(GA-1.)*RM+RM*.2.
C RETURN
C SNP55 SUBROUTINE SNP55(X1,X2,Y1,Y2)
C CALL SNP55(X1,X2,Y1,Y2)
C PLEAF1(W)
C END

C SNP55
C SUBROUTINE SNP55(X1,X2,Y1,Y2)
C X1=X(1)+X(2)/2
C X2=X(2)-X(1)/2.
C K1=1
C K2=2
C K3=3
C K4=4
C K5=5
C K6=6
C K7=7
C K8=8
C K9=9
C K10=10
C K11=11
C K12=12
C K13=13
C K14=14
C K15=15
C K16=16
C K17=17
C K18=18
C K19=19
C K20=20
C K21=21
C K22=22
C K23=23
C K24=24
C K25=25
C K26=26
C K27=27
C K28=28
C K29=29
C K30=30
C K31=31
C K32=32
C K33=33
C K34=34
C K35=35
C K36=36
C K37=37
C K38=38
C K39=39
C K40=40
C K41=41
C K42=42
C K43=43
C K44=44
C K45=45
C K46=46
C K47=47
C K48=48
C K49=49
C K50=50
C K51=51
C K52=52
C K53=53
C K54=54
C K55=55
C K56=56
C K57=57
C K58=58
C K59=59
C K60=60
C K61=61
C K62=62
C K63=63
C K64=64
C K65=65
C K66=66
C K67=67
C K68=68
C K69=69
C K70=70
C K71=71
C K72=72
C K73=73
C K74=74
C K75=75
C K76=76
C K77=77
C K78=78
C K79=79
C K80=80
C K81=81
C K82=82
C K83=83
C K84=84
C K85=85
C K86=86
C K87=87
C K88=88
C K89=89
C K90=90
C K91=91
C K92=92
C K93=93
C K94=94
C K95=95
C K96=96
C K97=97
C K98=98
C K99=99
C K100=100
C K101=101
C K102=102
C K103=103
C K104=104
C K105=105
C K106=106
C K107=107
C K108=108
C K109=109
C K110=110
C K111=111
C K112=112
C K113=113
C K114=114
C K115=115
C K116=116
C K117=117
C K118=118
C K119=119
C K120=120
C K121=121
C K122=122
C K123=123
C K124=124
C K125=125
C K126=126
C K127=127
C K128=128
C K129=129
C K130=130
C K131=131
C K132=132
C K133=133
C K134=134
C K135=135
C K136=136
C K137=137
C K138=138
C K139=139
C K140=140
C K141=141
C K142=142
C K143=143
C K144=144
C K145=145
C K146=146
C K147=147
C K148=148
C K149=149
C K150=150
C K151=151
C K152=152
C K153=153
C K154=154
C K155=155
C K156=156
C K157=157
C K158=158
C K159=159
C K160=160
C K161=161
C K162=162
C K163=163
C K164=164
C K165=165
C K166=166
C K167=167
C K168=168
C K169=169
C K170=170
C K171=171
C K172=172
C K173=173
C K174=174
C K175=175
C K176=176
C K177=177
C K178=178
C K179=179
C K180=180
C K181=181
C K182=182
C K183=183
C K184=184
C K185=185
C K186=186
C K187=187
C K188=188
C K189=189
C K190=190
C K191=191
C K192=192
C K193=193
C K194=194
C K195=195
C K196=196
C K197=197
C K198=198
C K199=199
C K200=200
C K201=201
C K202=202
C K203=203
C K204=204
C K205=205
C K206=206
C K207=207
C K208=208
C K209=209
C K210=210
C K211=211
C K212=212
C K213=213
C K214=214
C K215=215
C K216=216
C K217=217
C K218=218
C K219=219
C K220=220
C K221=221
C K222=222
C K223=223
C K224=224
C K225=225
C K226=226
C K227=227
C K228=228
C K229=229
C K230=230
C K231=231
C K232=232
C K233=233
C K234=234
C K235=235
C K236=236
C K237=237
C K238=238
C K239=239
C K240=240
C K241=241
C K242=242
C K243=243
C K244=244
C K245=245
C K246=246
C K247=247
C K248=248
C K249=249
C K250=250
C K251=251
C K252=252
C K253=253
C K254=254
C K255=255
C K256=256
C K257=257
C K258=258
C K259=259
C K260=260
C K261=261
C K262=262
C K263=263
C K264=264
C K265=265
C K266=266
C K267=267
C K268=268
C K269=269
C K270=270
C K271=271
C K272=272
C K273=273
C K274=274
C K275=275
C K276=276
C K277=277
C K278=278
C K279=279
C K280=280
C K281=281
C K282=282
C K283=283
C K284=284
C K285=285
C K286=286
C K287=287
C K288=288
C K289=289
C K290=290
C K291=291
C K292=292
C K293=293
C K294=294
C K295=295
C K296=296
C K297=297
C K298=298
C K299=299
C K300=300
C K301=301
C K302=302
C K303=303
C K304=304
C K305=305
C K306=306
C K307=307
C K308=308
C K309=309
C K310=310
C K311=311
C K312=312
C K313=313
C K314=314
C K315=315
C K316=316
C K317=317
C K318=318
C K319=319
C K320=320
C K321=321
C K322=322
C K323=323
C K324=324
C K325=325
C K326=326
C K327=327
C K328=328
C K329=329
C K330=330
C K331=331
C K332=332
C K333=333
C K334=334
C K335=335
C K336=336
C K337=337
C K338=338
C K339=339
C K340=340
C K341=341
C K342=342
C K343=343
C K344=344
C K345=345
C K346=346
C K347=347
C K348=348
C K349=349
C K350=350
C K351=351
C K352=352
C K353=353
C K354=354
C K355=355
C K356=356
C K357=357
C K358=358
C K359=359
C K360=360
C K361=361
C K362=362
C K363=363
C K364=364
C K365=365
C K366=366
C K367=367
C K368=368
C K369=369
C K370=370
C K371=371
C K372=372
C K373=373
C K374=374
C K375=375
C K376=376
C K377=377
C K378=378
C K379=379
C K380=380
C K381=381
C K382=382
C K383=383
C K384=384
C K385=385
C K386=386
C K387=387
C K388=388
C K389=389
C K390=390
C K391=391
C K392=392
C K393=393
C K394=394
C K395=395
C K396=396
C K397=397
C K398=398
C K399=399
C K400=400
C K401=401
C K402=402
C K403=403
C K404=404
C K405=405
C K406=406
C K407=407
C K408=408
C K409=409
C K410=410
C K411=411
C K412=412
C K413=413
C K414=414
C K415=415
C K416=416
C K417=417
C K418=418
C K419=419
C K420=420
C K421=421
C K422=422
C K423=423
C K424=424
C K425=425
C K426=426
C K427=427
C K428=428
C K429=429
C K430=430
C K431=431
C K432=432
C K433=433
C K434=434
C K435=435
C K436=436
C K437=437
C K438=438
C K439=439
C K440=440
C K441=441
C K442=442
C K443=443
C K444=444
C K445=445
C K446=446
C K447=447
C K448=448
C K449=449
C K450=450
C K451=451
C K452=452
C K453=453
C K454=454
C K455=455
C K456=456
C K457=457
C K458=458
C K459=459
C K460=460
C K461=461
C K462=462
C K463=463
C K464=464
C K465=465
C K466=466
C K467=467
C K468=468
C K469=469
C K470=470
C K471=471
C K472=472
C K473=473
C K474=474
C K475=475
C K476=476
C K477=477
C K478=478
C K479=479
C K480=480
C K481=481
C K482=482
C K483=483
C K484=484
C K485=485
C K486=486
C K487=487
C K488=488
C K489=489
C K490=490
C K491=491
C K492=492
C K493=493
C K494=494
C K495=495
C K496=496
C K497=497
C K498=498
C K499=499
C K500=500
C K501=501
C K502=502
C K503=503
C K504=504
C K505=505
C K506=506
C K507=507
C K508=508
C K509=509
C K510=510
C K511=511
C K512=512
C K513=513
C K514=514
C K515=515
C K516=516
C K517=517
C K518=518
C K519=519
C K520=520
C K521=521
C K522=522
C K523=523
C K524=524
C K525=525
C K526=526
C K527=527
C K528=528
C K529=529
C K530=530
C K531=531
C K532=532
C K533=533
C K534=534
C K535=535
C K536=536
C K537=537
C K538=538
C K539=539
C K540=540
C K541=541
C K542=542
C K543=543
C K544=544
C K545=545
C K546=546
C K547=547
C K548=548
C K549=549
C K550=550
C K551=551
C K552=552
C K553=553
C K554=554
C K555=555
C K556=556
C K557=557
C K558=558
C K559=559
C K560=560
C K561=561
C K562=562
C K563=563
C K564=564
C K565=565
C K566=566
C K567=567
C K568=568
C K569=569
C K570=570
C K571=571
C K572=572
C K573=573
C K574=574
C K575=575
C K576=576
C K577=577
C K578=578
C K579=579
C K580=580
C K581=581
C K582=582
C K583=583
C K584=584
C K585=585
C K586=586
C K587=587
C K588=588
C K589=589
C K590=590
C K591=591
C K592=592
C K593=593
C K594=594
C K595=595
C K596=596
C K597=597
C K598=598
C K599=599
C K600=600
C K601=601
C K602=602
C K603=603
C K604=604
C K605=605
C K606=606
C K607=607
C K608=608
C K609=609
C K610=610
C K611=611
C K612=612
C K613=613
C K614=614
C K615=615
C K616=616
C K617=617
C K618=618
C K619=619
C K620=620
C K621=621
C K622=622
C K623=623
C K624=624
C K625=625
C K626=626
C K627=627
C K628=628
C K629=629
C K630=630
C K631=631
C K632=632
C K633=633
C K634=634
C K635=635
C K636=636
C K637=637
C K638=638
C K639=639
C K640=640
C K641=641
C K642=642
C K643=643
C K644=644
C K645=645
C K646=646
C K647=647
C K648=648
C K649=649
C K650=650
C K651=651
C K652=652
C K653=653
C K654=654
C K655=655
C K656=656
C K657=657
C K658=658
C K659=659
C K660=660
C K661=661
C K662=662
C K663=663
C K664=664
C K665=665
C K666=666
C K667=667
C K668=668
C K669=669
C K670=670
C K671=671
C K672=672
C K673=673
C K674=674
C K675=675
C K676=676
C K677=677
C K678=678
C K679=679
C K680=680
C K681=681
C K682=682
C K683=683
C K684=684
C K685=685
C K686=686
C K687=687
C K688=688
C K689=689
C K690=690
C K691=691
C K692=692
C K693=693
C K694=694
C K695=695
C K696=696
C K697=697
C K698=698
C K699=699
C K700=700
C K701=701
C K702=702
C K703=703
C K704=704
C K705=705
C K706=706
C K707=707
C K708=708
C K709=709
C K710=710
C K711=711
C K712=712
C K713=713
C K714=714
C K715=715
C K716=716
C K717=717
C K718=718
C K719=719
C K720=720
C K721=721
C K722=722
C K723=723
C K724=724
C K725=725
C K726=726
C K727=727
C K728=728
C K729=729
C K730=730
C K731=731
C K732=732
C K733=733
C K734=734
C K735=735
C K736=736
C K737=737
C K738=738
C K739=739
C K740=740
C K741=741
C K742=742
C K743=743
C K744=744
C K745=745
C K746=746
C K747=747
C K748=748
C K749=749
C K750=750
C K751=751
C K752=752
C K753=753
C K754=754
C K755=755
C K756=756
C K757=757
C K758=758
C K759=759
C K760=760
C K761=761
C K762=762
C K763=763
C K764=764
C K765=765
C K766=766
C K767=767
C K768=768
C K769=769
C K770=770
C K771=771
C K772=772
C K773=773
C K774=774
C K775=775
C K776=776
C K777=777
C K778=778
C K779=779
C K780=780
C K781=781
C K782=782
C K783=783
C K784=784
C K785=785
C K786=786
C K787=787
C K788=788
C K789=789
C K790=790
C K791=791
C K792=792
C K793=793
C K794=794
C K795=795
C K796=796
C K797=797
C K798=798
C K799=799
C K800=800
C K801=801
C K802=802
C K803=803
C K804=804
C K805=805
C K806=806
C K807=807
C K808=808
C K809=809
C K810=810
C K811=811
C K812=812
C K813=813
C K814=814
C K815=815
C K816=816
C K817=817
C K818=818
C K819=819
C K820=820
C K821=821
C K822=822
C K823=823
C K824=824
C K825=825
C K826=826
C K827=827
C K828=828
C K829=829
C K830=830
C K831=831
C K832=832
C K833=833
C K834=834
C K835=835
C K836=836
C K837=837
C K838=838
C K839=839
C K840=840
C K841=841
C K842=842
C K843=843
C K844=844
C K845=845
C K846=846
C K847=847
C K848=848
C K849=849
C K850=850
C K851=851
C K852=852
C K853=853
C K854=854
C K855=855
C K856=856
C K857=857
C K858=858
C K859=859
C K860=860
C K861=861
C K862=862
C K863=863
C K864=864
C K865=865
C K866=866
C K867=867
C K868=868
C K869=869
C K870=870
C K871=871
C K872=872
C K873=873
C K874=874
C K875=875
C K876=876
C K877=877
C K878=878
C K879=879
C K880=880
C K881=881
C K882=882
C K883=883
C K884=884
C K885=885
C K886=886
C K887=887
C K888=888
C K889=889
C K890=890
C K891=891
C K892=892
C K893=893
C K894=894
C K895=895
C K896=896
C K897=897
C K898=898
C K899=899
C K900=900
C K901=901
C K902=902
C K903=903
C K904=904
C K905=905
C K906=906
C K907=907
C K908=908
C K909=909
C K910=910
C K911=911
C K912=912
C K913=913
C K914=914
C K915=915
C K916=916
C K917=917
C K918=918
C K919=919
C K920=920
C K921=921
C K922=922
C K923=923
C K924=924
C K925=925
C K926=926
C K927=927
C K928=928
C K929=929
C K930=930
C K931=931
C K932=932
C K933=933
C K934=934
C K935=935
C K936=936
C K937=937
C K938=938
C K939=939
C K940=940
C K941=941
C K942=942
C K943=943
C K944=944
C K945=945
C K946=946
C K947=947
C K948=948
C K949=949
C K950=950
C K951=951
C K952=952
C K953=953
C K954=954
C K955=955
C K956=956
C K957=957
C K958=958
C K959=959
C K960=960
C K961=961
C K962=962
C K963=963
C K964=964
C K965=965
C K966=966
C K967=967
C K968=968
C K969=969
C K970=970
C K971=971
C K972=972
C K973=973
C K974=974
C K975=975
C K976=976
C K977=977
C K978=978
C K979=979
C K980=980
C K981=981
C K982=982
C K983=983
C K984=984
C K985=985
C K986=986
C K987=987
C K988=988
C K989=989
C K990=990
C K991=991
C K992=992
C K993=993
C K994=994
C K995=995
C K996=996
C K997=997
C K998=998
C K999=999
C K1000=1000
C K1001=1001
C K1002=1002
C K1003=1003
C K1004=1004
C K1005=1005
C K1006=1006
C K1007=1007
C K1008=1008
C K1009=1009
C K1010=1010
C K1011=1011
C K1012=1012
C K1013=1013
C K1014=1014
C K1015=1015
C K1016=1016
C K1017=1017
C K1018=1018
C K1019=1019
C K1020=1020
C K1021=1021
C K1022=1022
C K1023=1023
C K1024=1024
C K1025=1025
C K1026=1026
C K1027=1027
C K1028=1028
C K1029=1029
C K1030=1030
C K1031=1031
C K1032=1032
C K1033=1033
C K1034=1034
C K1035=1035
C K1036=1036
C K1037=1037
C K1038=1038
C K1039=1039
C K1040=1040
C K1041=1041
C K1042=1042
C K1043=1043
C K1044=1044
C K1045=1045
C K1046=1046
C K1047=1047
C K1048=1048
C K1049=1049
C K1050=1050
C K1051=1051
C K1052=1052
C K1053=1053
C K1054=1054
C K1055=1055
C K1056=1056
C K1057=1057
C K1058=1058
C K1059=1059
C K1060=1060
C K1061=1061
C K1062=1062
C K1063=1063
C K1064=1064
C K1065=1065
C K1066=1066
C K1067=1067
C K1068=1068
C K1069=1069
C K1070=1070
C K1071=1071
C K1072=1072
C K1073=1073
C K1074=1074
C K1075=1075
C K1076=1076
C K1077=1077
C K1078=1078
C K1079=1079
C K1080=1080
C K1081=1081
C K1082=1082
C K1083=1083
C K1084=1084
C K1085=1085
C K1086=1086
C K1087=1087
C K1088=1088
C K1089=1089
C K1090=1090
C K1091=1091
C K1092=1092
C K1093=1093
C K1094=1094
C K1095=1095
C K1096=1096
C K1097=1097
C K1098=1098
C K1099=1099
C K1100=1100
C K1101=1101
C K1102=1102
C K1103=1103
C K1104=1104
C K1105=1105
C K1106=1106
C K1107=1107
C K1108=1108
C K1109=1109
C K1110
```

CFCL IN

356
357
358
359
360
361
362
363
364
365
366
367
368
369
370
371
372
373
374
375
376
377
378
379
380
381
382
383
384
385
386
387
388
389
390
391
392
393
394
395
396
397
398
399
400
401
402
403
404
405
406
407
408
409
410
411
412
413
414
415
416
417
418
419
420
421
422
423
424
425
426
427
428
429
430
431
432
433
434
435
436
437
438
439
440
441
442
443
444
445
446
447
448
449
450
451
452
453
454
455
456
457
458
459
460
461
462
463
464
465
466
467
468
469
470
471
472
473
474
475
476
477
478
479
480
481
482
483
484
485
486
487
488
489
490
491
492
493
494
495
496
497
498
499
500
501
502
503
504
505
506
507
508
509
510
511
512
513
514
515
516
517
518
519
520
521
522
523
524
525
526
527
528
529
530
531
532
533
534
535
536
537
538
539
540
541
542
543
544
545
546
547
548
549
550
551
552
553
554
555
556
557
558
559
559
560
561
562
563
564
565
566
567
568
569
569
570
571
572
573
574
575
576
577
578
579
579
580
581
582
583
584
585
586
587
588
589
589
590
591
592
593
594
595
596
597
598
599
599
600
601
602
603
604
605
606
607
608
609
609
610
611
612
613
614
615
616
617
618
619
619
620
621
622
623
624
625
626
627
628
629
629
630
631
632
633
634
635
636
637
638
639
639
640
641
642
643
644
645
646
647
648
649
649
650
651
652
653
654
655
656
657
658
659
659
660
661
662
663
664
665
666
667
668
669
669
670
671
672
673
674
675
676
677
678
679
679
680
681
682
683
684
685
686
687
688
689
689
690
691
692
693
694
695
696
697
698
699
699
700
701
702
703
704
705
706
707
708
709
709
710
711
712
713
714
715
716
717
718
719
719
720
721
722
723
724
725
726
727
728
729
729
730
731
732
733
734
735
736
737
738
739
739
740
741
742
743
744
745
746
747
748
749
749
750
751
752
753
754
755
756
757
758
759
759
760
761
762
763
764
765
766
767
768
769
769
770
771
772
773
774
775
776
777
778
779
779
780
781
782
783
784
785
786
787
788
789
789
790
791
792
793
794
795
796
797
798
799
799
800
801
802
803
804
805
806
807
808
809
809
810
811
812
813
814
815
816
817
818
819
819
820
821
822
823
824
825
826
827
828
829
829
830
831
832
833
834
835
836
837
838
839
839
840
841
842
843
844
845
846
847
848
849
849
850
851
852
853
854
855
856
857
858
859
859
860
861
862
863
864
865
866
867
868
869
869
870
871
872
873
874
875
876
877
878
879
879
880
881
882
883
884
885
886
887
888
889
889
890
891
892
893
894
895
896
897
898
899
899
900
901
902
903
904
905
906
907
908
909
909
910
911
912
913
914
915
916
917
918
919
919
920
921
922
923
924
925
926
927
928
929
929
930
931
932
933
934
935
936
937
938
939
939
940
941
942
943
944
945
946
947
948
949
949
950
951
952
953
954
955
956
957
958
959
959
960
961
962
963
964
965
966
967
968
969
969
970
971
972
973
974
975
976
977
978
979
979
980
981
982
983
984
985
986
987
988
989
989
990
991
992
993
994
995
996
997
998
999
999
1000

.....

6. 0000048
 0. 0261745
 0. 0156273
 0. 0142056
 0. 0138056
 0. 0134056
 0. 0130056
 0. 0126056
 0. 0122056
 0. 0118056
 0. 0114056
 0. 0110056
 0. 0106056
 0. 0102056
 0. 0108056
 0. 0104056
 0. 0100056
 0. 0096056
 0. 0092056
 0. 0088056
 0. 0084056
 0. 0080056
 0. 0076056
 0. 0072056
 0. 0068056
 0. 0064056
 0. 0060056
 0. 0056056
 0. 0052056
 0. 0048056
 0. 0044056
 0. 0040056
 0. 0036056
 0. 0032056
 0. 0028056
 0. 0024056
 0. 0020056
 0. 0016056
 0. 0012056
 0. 0008056
 0. 0004056
 0. 0000056

101

ACA 2112 TEST CASE
LAKE COTTAGEIES AND DERIV

CFC2 OUT

NACA 2412 TEST CASE E
T₂ = 6.2 m³/s ELS = 0.07448 Hz = 64

INLET CONDITIONS

E₁ = 21.35 m^{1/4} E₂ = 1.00897
OUTLET CONDITIONS
E₂ = 7.21 m^{1/4} = 0.94719

NON DIMENSIONAL CIRCULATION = -1.30829

THE 2-D LIFT COEFFICIENT = 2.61659

THE 2-D PITCHING MOMENT COEFFICIENT = -0.0003540

VELOCITY DISTRIBUTION

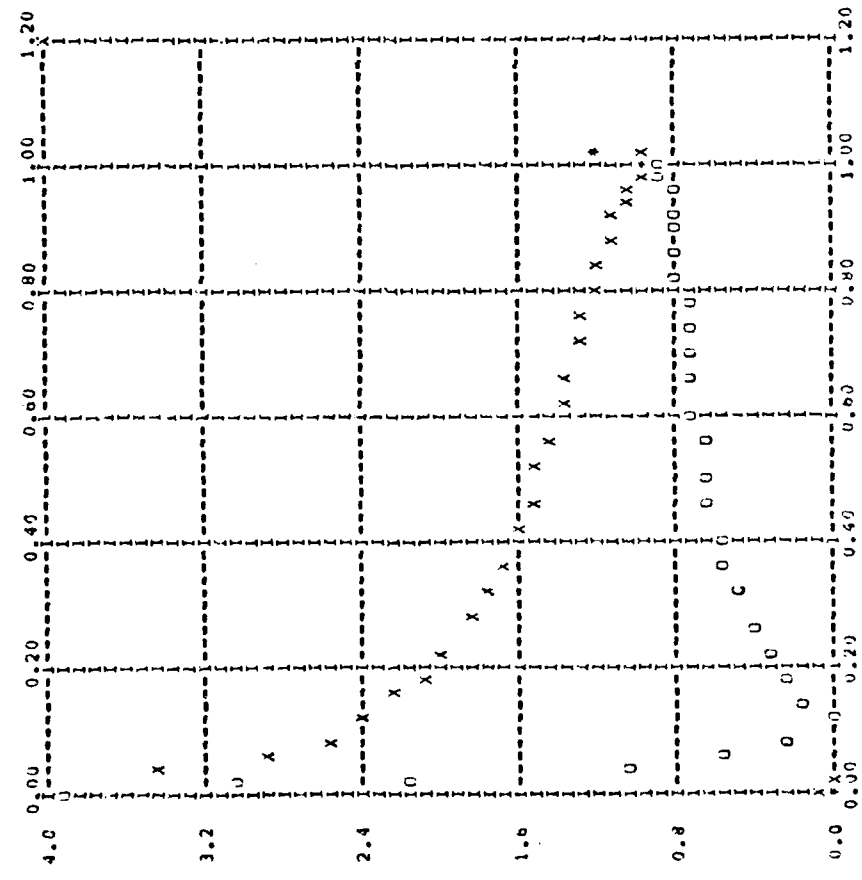
PRESSURE SIDE

X/C	SUCTION SIDE	W/L/WI	X/C	PRESSURE SIDE	W/L/WI
0.000	0.000	-1.113	0.000	0.000	-1.113
0.004	0.003	-0.439	0.001	0.003	-0.439
0.004	0.010	-1.024	0.005	0.012	-1.024
0.011	0.022	-1.253	0.014	0.022	-1.253
0.021	0.031	-1.417	0.029	0.034	-1.417
0.031	0.031	-1.491	0.041	0.034	-1.491
0.041	0.031	-1.560	0.052	0.034	-1.560
0.051	0.031	-1.620	0.062	0.034	-1.620
0.061	0.031	-1.669	0.072	0.034	-1.669
0.071	0.031	-1.707	0.081	0.034	-1.707
0.081	0.031	-1.735	0.091	0.034	-1.735
0.091	0.031	-1.753	0.101	0.034	-1.753
0.101	0.031	-1.761	0.111	0.034	-1.761
0.111	0.031	-1.769	0.121	0.034	-1.769
0.121	0.031	-1.775	0.131	0.034	-1.775
0.131	0.031	-1.780	0.141	0.034	-1.780
0.141	0.031	-1.784	0.151	0.034	-1.784
0.151	0.031	-1.787	0.161	0.034	-1.787
0.161	0.031	-1.790	0.171	0.034	-1.790
0.171	0.031	-1.792	0.181	0.034	-1.792
0.181	0.031	-1.794	0.191	0.034	-1.794
0.191	0.031	-1.795	0.201	0.034	-1.795
0.201	0.031	-1.796	0.211	0.034	-1.796
0.211	0.031	-1.797	0.221	0.034	-1.797
0.221	0.031	-1.798	0.231	0.034	-1.798
0.231	0.031	-1.798	0.241	0.034	-1.798
0.241	0.031	-1.798	0.251	0.034	-1.798
0.251	0.031	-1.798	0.261	0.034	-1.798
0.261	0.031	-1.798	0.271	0.034	-1.798
0.271	0.031	-1.798	0.281	0.034	-1.798
0.281	0.031	-1.798	0.291	0.034	-1.798
0.291	0.031	-1.798	0.301	0.034	-1.798
0.301	0.031	-1.798	0.311	0.034	-1.798
0.311	0.031	-1.798	0.321	0.034	-1.798
0.321	0.031	-1.798	0.331	0.034	-1.798
0.331	0.031	-1.798	0.341	0.034	-1.798
0.341	0.031	-1.798	0.351	0.034	-1.798
0.351	0.031	-1.798	0.361	0.034	-1.798
0.361	0.031	-1.798	0.371	0.034	-1.798
0.371	0.031	-1.798	0.381	0.034	-1.798
0.381	0.031	-1.798	0.391	0.034	-1.798
0.391	0.031	-1.798	0.401	0.034	-1.798
0.401	0.031	-1.798	0.411	0.034	-1.798
0.411	0.031	-1.798	0.421	0.034	-1.798
0.421	0.031	-1.798	0.431	0.034	-1.798
0.431	0.031	-1.798	0.441	0.034	-1.798
0.441	0.031	-1.798	0.451	0.034	-1.798
0.451	0.031	-1.798	0.461	0.034	-1.798
0.461	0.031	-1.798	0.471	0.034	-1.798
0.471	0.031	-1.798	0.481	0.034	-1.798
0.481	0.031	-1.798	0.491	0.034	-1.798
0.491	0.031	-1.798	0.501	0.034	-1.798
0.501	0.031	-1.798	0.511	0.034	-1.798
0.511	0.031	-1.798	0.521	0.034	-1.798
0.521	0.031	-1.798	0.531	0.034	-1.798
0.531	0.031	-1.798	0.541	0.034	-1.798
0.541	0.031	-1.798	0.551	0.034	-1.798
0.551	0.031	-1.798	0.561	0.034	-1.798
0.561	0.031	-1.798	0.571	0.034	-1.798
0.571	0.031	-1.798	0.581	0.034	-1.798
0.581	0.031	-1.798	0.591	0.034	-1.798
0.591	0.031	-1.798	0.601	0.034	-1.798
0.601	0.031	-1.798	0.611	0.034	-1.798
0.611	0.031	-1.798	0.621	0.034	-1.798
0.621	0.031	-1.798	0.631	0.034	-1.798
0.631	0.031	-1.798	0.641	0.034	-1.798
0.641	0.031	-1.798	0.651	0.034	-1.798
0.651	0.031	-1.798	0.661	0.034	-1.798
0.661	0.031	-1.798	0.671	0.034	-1.798
0.671	0.031	-1.798	0.681	0.034	-1.798
0.681	0.031	-1.798	0.691	0.034	-1.798
0.691	0.031	-1.798	0.701	0.034	-1.798
0.701	0.031	-1.798	0.711	0.034	-1.798
0.711	0.031	-1.798	0.721	0.034	-1.798
0.721	0.031	-1.798	0.731	0.034	-1.798
0.731	0.031	-1.798	0.741	0.034	-1.798
0.741	0.031	-1.798	0.751	0.034	-1.798
0.751	0.031	-1.798	0.761	0.034	-1.798
0.761	0.031	-1.798	0.771	0.034	-1.798
0.771	0.031	-1.798	0.781	0.034	-1.798
0.781	0.031	-1.798	0.791	0.034	-1.798
0.791	0.031	-1.798	0.801	0.034	-1.798
0.801	0.031	-1.798	0.811	0.034	-1.798
0.811	0.031	-1.798	0.821	0.034	-1.798
0.821	0.031	-1.798	0.831	0.034	-1.798
0.831	0.031	-1.798	0.841	0.034	-1.798
0.841	0.031	-1.798	0.851	0.034	-1.798
0.851	0.031	-1.798	0.861	0.034	-1.798
0.861	0.031	-1.798	0.871	0.034	-1.798
0.871	0.031	-1.798	0.881	0.034	-1.798
0.881	0.031	-1.798	0.891	0.034	-1.798
0.891	0.031	-1.798	0.901	0.034	-1.798
0.901	0.031	-1.798	0.911	0.034	-1.798
0.911	0.031	-1.798	0.921	0.034	-1.798
0.921	0.031	-1.798	0.931	0.034	-1.798
0.931	0.031	-1.798	0.941	0.034	-1.798
0.941	0.031	-1.798	0.951	0.034	-1.798
0.951	0.031	-1.798	0.961	0.034	-1.798
0.961	0.031	-1.798	0.971	0.034	-1.798
0.971	0.031	-1.798	0.981	0.034	-1.798
0.981	0.031	-1.798	0.991	0.034	-1.798
0.991	0.031	-1.798	0.998	0.034	-1.798

CFC2 OUT					
(P01-P51)/01 DISTRIBUTION					
X/C SUCTION SIDE S LOC					
ML	LOC	S LOC	S/C	PRESSURE SIDE	X/C
0.000	0.000	0.000	1.23	0.44	-1.113
0.013	0.013	0.013	1.15	0.537	-1.072
0.022	0.022	0.022	1.09	0.622	-1.034
0.039	0.039	0.039	1.04	0.523	-1.024
0.050	0.050	0.050	1.01	0.523	-1.024
0.061	0.061	0.061	0.98	0.523	-1.024
0.071	0.071	0.071	0.96	0.523	-1.024
0.081	0.081	0.081	0.94	0.523	-1.024
0.091	0.091	0.091	0.93	0.523	-1.024
0.101	0.101	0.101	0.92	0.523	-1.024
0.111	0.111	0.111	0.91	0.523	-1.024
0.121	0.121	0.121	0.90	0.523	-1.024
0.131	0.131	0.131	0.89	0.523	-1.024
0.141	0.141	0.141	0.88	0.523	-1.024
0.151	0.151	0.151	0.87	0.523	-1.024
0.161	0.161	0.161	0.86	0.523	-1.024
0.171	0.171	0.171	0.85	0.523	-1.024
0.181	0.181	0.181	0.84	0.523	-1.024
0.191	0.191	0.191	0.83	0.523	-1.024
0.201	0.201	0.201	0.82	0.523	-1.024
0.211	0.211	0.211	0.81	0.523	-1.024
0.221	0.221	0.221	0.80	0.523	-1.024
0.231	0.231	0.231	0.79	0.523	-1.024
0.241	0.241	0.241	0.78	0.523	-1.024
0.251	0.251	0.251	0.77	0.523	-1.024
0.261	0.261	0.261	0.76	0.523	-1.024
0.271	0.271	0.271	0.75	0.523	-1.024
0.281	0.281	0.281	0.74	0.523	-1.024
0.291	0.291	0.291	0.73	0.523	-1.024
0.301	0.301	0.301	0.72	0.523	-1.024
0.311	0.311	0.311	0.71	0.523	-1.024
0.321	0.321	0.321	0.70	0.523	-1.024
0.331	0.331	0.331	0.69	0.523	-1.024
0.341	0.341	0.341	0.68	0.523	-1.024
0.351	0.351	0.351	0.67	0.523	-1.024
0.361	0.361	0.361	0.66	0.523	-1.024
0.371	0.371	0.371	0.65	0.523	-1.024
0.381	0.381	0.381	0.64	0.523	-1.024
0.391	0.391	0.391	0.63	0.523	-1.024
0.401	0.401	0.401	0.62	0.523	-1.024
0.411	0.411	0.411	0.61	0.523	-1.024
0.421	0.421	0.421	0.60	0.523	-1.024
0.431	0.431	0.431	0.59	0.523	-1.024
0.441	0.441	0.441	0.58	0.523	-1.024
0.451	0.451	0.451	0.57	0.523	-1.024
0.461	0.461	0.461	0.56	0.523	-1.024
0.471	0.471	0.471	0.55	0.523	-1.024
0.481	0.481	0.481	0.54	0.523	-1.024
0.491	0.491	0.491	0.53	0.523	-1.024
0.501	0.501	0.501	0.52	0.523	-1.024
0.511	0.511	0.511	0.51	0.523	-1.024
0.521	0.521	0.521	0.50	0.523	-1.024
0.531	0.531	0.531	0.49	0.523	-1.024
0.541	0.541	0.541	0.48	0.523	-1.024

NACA 2412 TEST CASE
 $\bar{t} = 0.28319$ ELE = 0.07418 RE = 64

PLUT MACH NUMBER DISTRIBUTION



CFC3 OUT

MAGNATION POINT IS AT θ X = 0.10466
 SECTION SIDE SEPARATION POINT IS θ 57 S/C = 0.15066

MAGNATION POINT IS AT θ X = 0.16466
 PRESSURE SIDE SEPARATION POINT IS θ 33 S/C = 1.02761

OF ATTACK = 0.349

K CF ITERATIONS = 0

LATIION = -0.69835

-0 LIFT COEFFICIENT = 1.39671

-0 FLOW DRAG COEFFICIENT = 0.64329350

-0 FRICTION DRAG COEFFICIENT = 0.00000000

-0 PITCHING MOMENT COEFFICIENT = -0.0303974

MIXY DISTRIBUTION

	FRICITION SIDE	S/C	X/L/W1	PRESSURE SIDE	S/C	X/L/W1
0.0	0.000	-7.100	0.000	0.000	-7.100	0.000
0.1	0.000	-2.893	0.001	0.003	-2.469	0.003
0.2	0.010	-2.741	0.003	0.010	-2.415	0.010
0.3	0.022	-3.010	0.013	0.022	-2.670	0.022
0.4	0.039	-2.480	0.029	0.039	-3.346	0.039
0.5	0.053	-2.158	0.051	0.053	-3.001	0.051
0.6	0.067	-1.961	0.075	0.067	-2.614	0.075
0.7	0.081	-1.712	0.092	0.081	-2.214	0.092
0.8	0.095	-1.515	0.109	0.095	-1.790	0.109
0.9	0.107	-1.343	0.125	0.107	-1.327	0.125
1.0	0.120	-1.214	0.135	0.120	-1.213	0.135

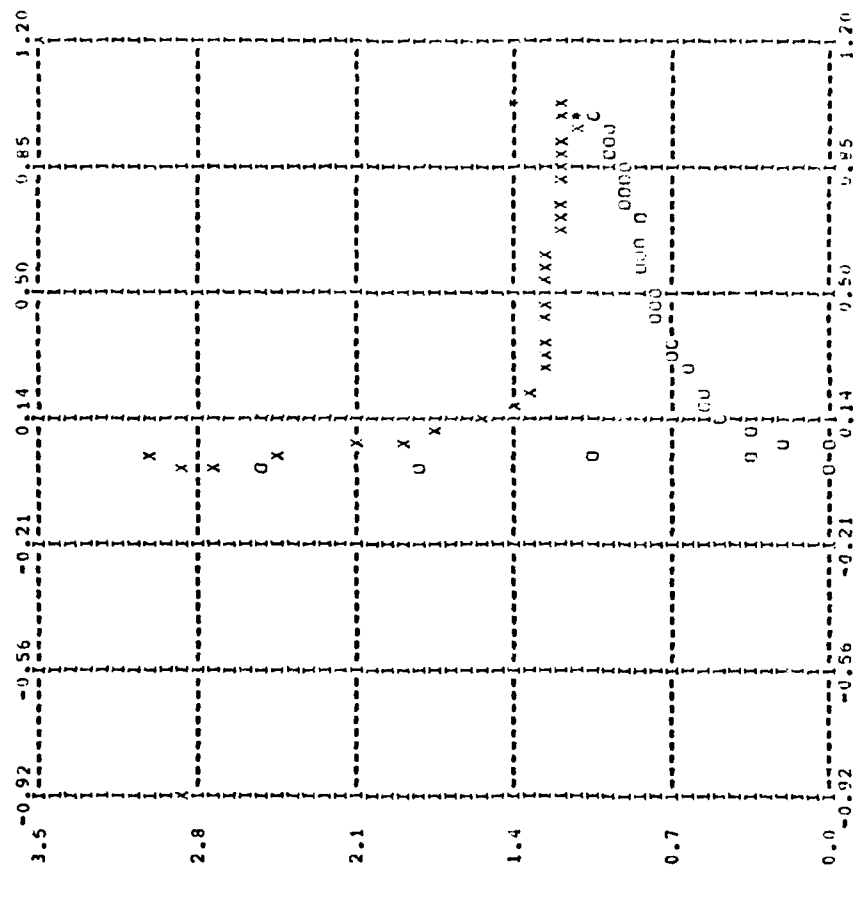
	FRICITION SIDE	S/C	X/L/W1	PRESSURE SIDE	S/C	X/L/W1
0.0	0.000	-7.100	0.000	0.000	-7.100	0.000
0.1	0.000	-2.893	0.001	0.003	-2.469	0.003
0.2	0.010	-2.741	0.003	0.010	-2.415	0.010
0.3	0.022	-3.010	0.013	0.022	-2.670	0.022
0.4	0.039	-2.480	0.029	0.039	-3.346	0.039
0.5	0.053	-2.158	0.051	0.053	-3.001	0.051
0.6	0.067	-1.961	0.075	0.067	-2.614	0.075
0.7	0.081	-1.712	0.092	0.081	-2.214	0.092
0.8	0.095	-1.515	0.109	0.095	-1.790	0.109
0.9	0.107	-1.343	0.125	0.107	-1.327	0.125
1.0	0.120	-1.214	0.135	0.120	-1.213	0.135

2412 TEST CASE
.28319 F.L.= 0.07448 N= 64

SL/SC DISTRIBUTION

S/SC	S LOC	PRESSURE SIDE	S LOC
X/C		X/C	
0.0	51.353	0.4000	51.353
0.1	51.398	0.4001	51.398
0.4	51.515	0.4005	51.515
1.1	51.622	0.4012	51.622
1.4	51.639	0.4013	51.639
1.8	51.656	0.4014	51.656
2.1	51.673	0.4015	51.673
2.4	51.689	0.4016	51.689
2.7	51.706	0.4017	51.706
3.0	51.723	0.4018	51.723
3.3	51.739	0.4019	51.739
3.6	51.756	0.4020	51.756
3.9	51.772	0.4021	51.772
4.2	51.789	0.4022	51.789
4.5	51.805	0.4023	51.805
4.8	51.821	0.4024	51.821
5.1	51.837	0.4025	51.837
5.4	51.853	0.4026	51.853
5.7	51.869	0.4027	51.869
6.0	51.885	0.4028	51.885
6.3	51.901	0.4029	51.901
6.6	51.917	0.4030	51.917
6.9	51.933	0.4031	51.933
7.2	51.949	0.4032	51.949
7.5	51.965	0.4033	51.965
7.8	51.981	0.4034	51.981
8.1	51.997	0.4035	51.997
8.4	52.013	0.4036	52.013
8.7	52.029	0.4037	52.029
9.0	52.045	0.4038	52.045
9.3	52.061	0.4039	52.061
9.6	52.077	0.4040	52.077
9.9	52.093	0.4041	52.093
10.2	52.109	0.4042	52.109
10.5	52.125	0.4043	52.125
10.8	52.141	0.4044	52.141
11.1	52.157	0.4045	52.157
11.4	52.173	0.4046	52.173
11.7	52.189	0.4047	52.189
12.0	52.205	0.4048	52.205
12.3	52.221	0.4049	52.221
12.6	52.237	0.4050	52.237
12.9	52.253	0.4051	52.253
13.2	52.269	0.4052	52.269
13.5	52.285	0.4053	52.285
13.8	52.301	0.4054	52.301
14.1	52.317	0.4055	52.317
14.4	52.333	0.4056	52.333
14.7	52.349	0.4057	52.349
15.0	52.365	0.4058	52.365
15.3	52.381	0.4059	52.381
15.6	52.397	0.4060	52.397
15.9	52.413	0.4061	52.413
16.2	52.429	0.4062	52.429
16.5	52.445	0.4063	52.445
16.8	52.461	0.4064	52.461
17.1	52.477	0.4065	52.477
17.4	52.493	0.4066	52.493
17.7	52.509	0.4067	52.509
18.0	52.525	0.4068	52.525
18.3	52.541	0.4069	52.541
18.6	52.557	0.4070	52.557
18.9	52.573	0.4071	52.573
19.2	52.589	0.4072	52.589
19.5	52.605	0.4073	52.605
19.8	52.621	0.4074	52.621
20.1	52.637	0.4075	52.637
20.4	52.653	0.4076	52.653
20.7	52.669	0.4077	52.669
21.0	52.685	0.4078	52.685
21.3	52.701	0.4079	52.701
21.6	52.717	0.4080	52.717
21.9	52.733	0.4081	52.733
22.2	52.749	0.4082	52.749
22.5	52.765	0.4083	52.765
22.8	52.781	0.4084	52.781
23.1	52.797	0.4085	52.797
23.4	52.813	0.4086	52.813
23.7	52.829	0.4087	52.829
24.0	52.845	0.4088	52.845
24.3	52.861	0.4089	52.861
24.6	52.877	0.4090	52.877
24.9	52.893	0.4091	52.893
25.2	52.909	0.4092	52.909
25.5	52.925	0.4093	52.925
25.8	52.941	0.4094	52.941
26.1	52.957	0.4095	52.957
26.4	52.973	0.4096	52.973
26.7	52.989	0.4097	52.989
27.0	53.005	0.4098	53.005
27.3	53.021	0.4099	53.021
27.6	53.037	0.4100	53.037
27.9	53.053	0.4101	53.053
28.2	53.069	0.4102	53.069
28.5	53.085	0.4103	53.085
28.8	53.101	0.4104	53.101
29.1	53.117	0.4105	53.117
29.4	53.133	0.4106	53.133
29.7	53.149	0.4107	53.149
30.0	53.165	0.4108	53.165
30.3	53.181	0.4109	53.181
30.6	53.197	0.4110	53.197
30.9	53.213	0.4111	53.213
31.2	53.229	0.4112	53.229
31.5	53.245	0.4113	53.245
31.8	53.261	0.4114	53.261
32.1	53.277	0.4115	53.277
32.4	53.293	0.4116	53.293
32.7	53.309	0.4117	53.309
33.0	53.325	0.4118	53.325
33.3	53.341	0.4119	53.341
33.6	53.357	0.4120	53.357

NON DIMENSIONAL VELOCITY DISTRIBUTION



THE MODEL

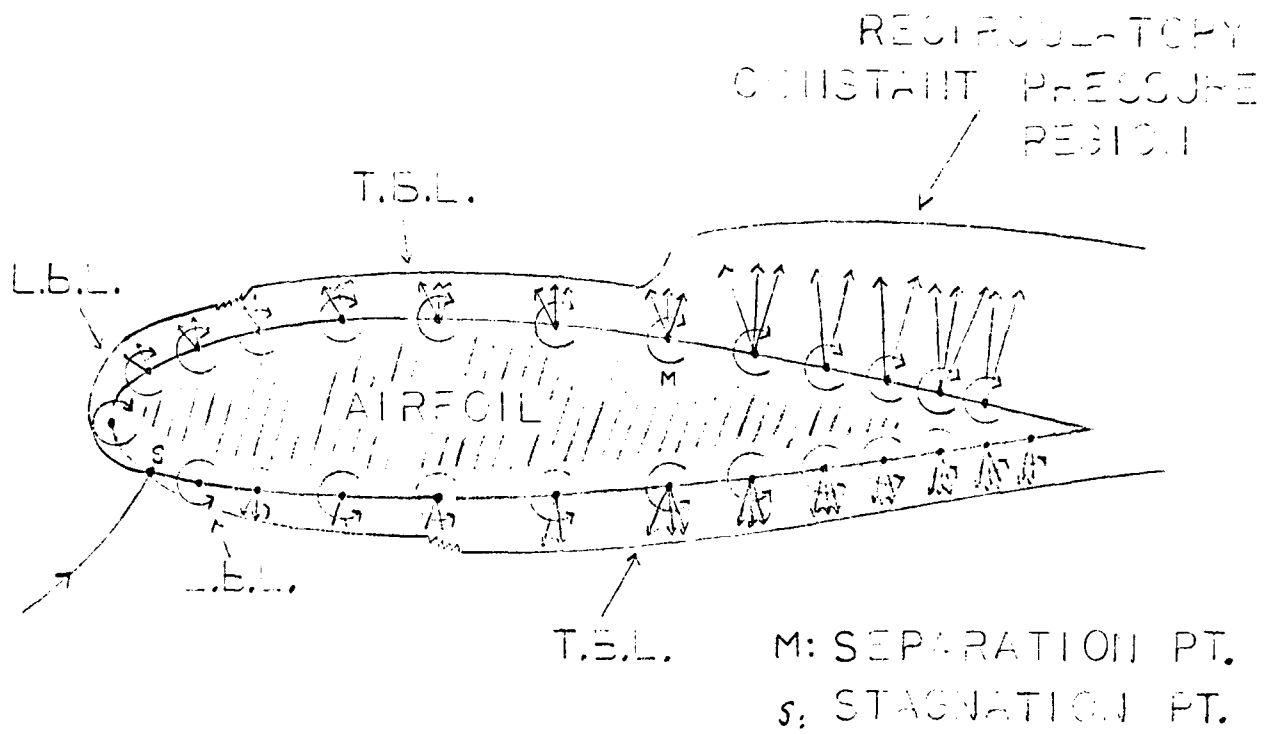


Fig. 1. The Model

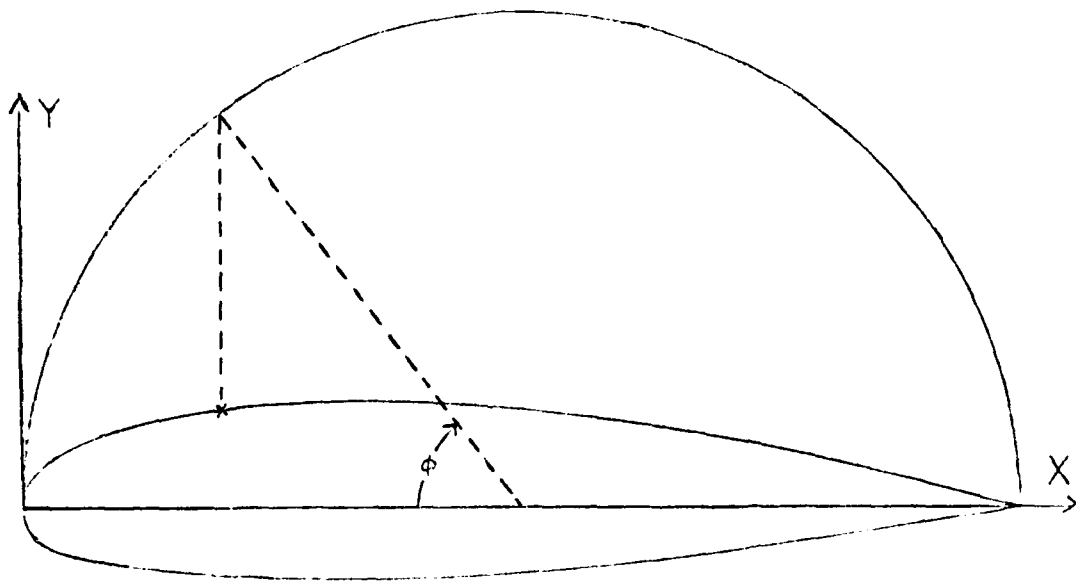


Fig. 2. The Airfoil Coordinate System

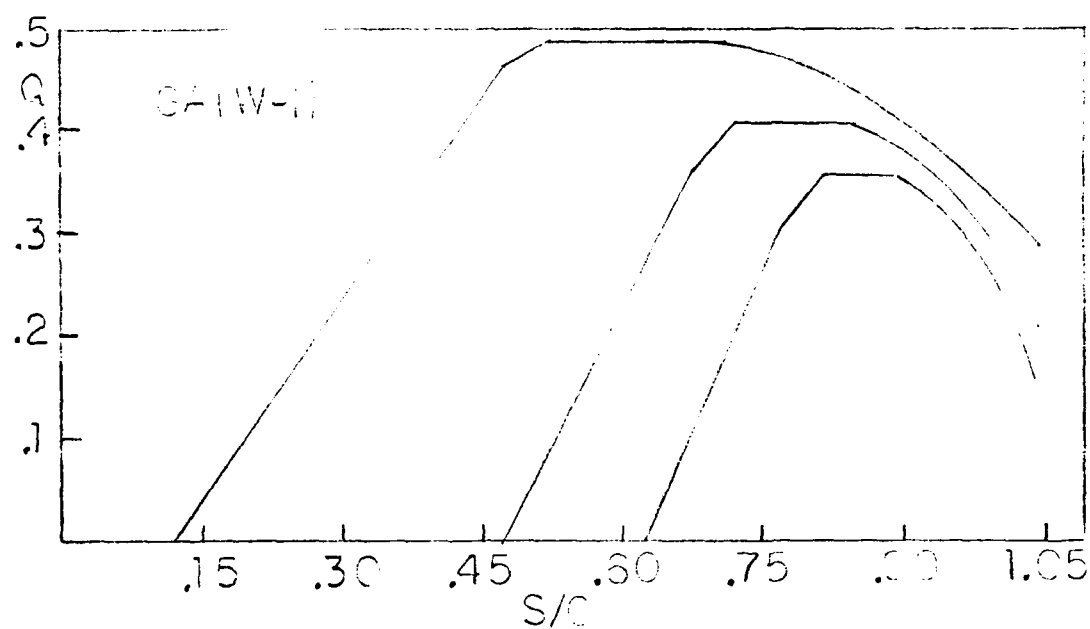


Fig. 3. Source Distributions for the GA(W-1)

THE COMPUTER PROGRAM

THE FLOW CHART ILLUSTRATES THE COMPUTATIONAL PROCEDURE.

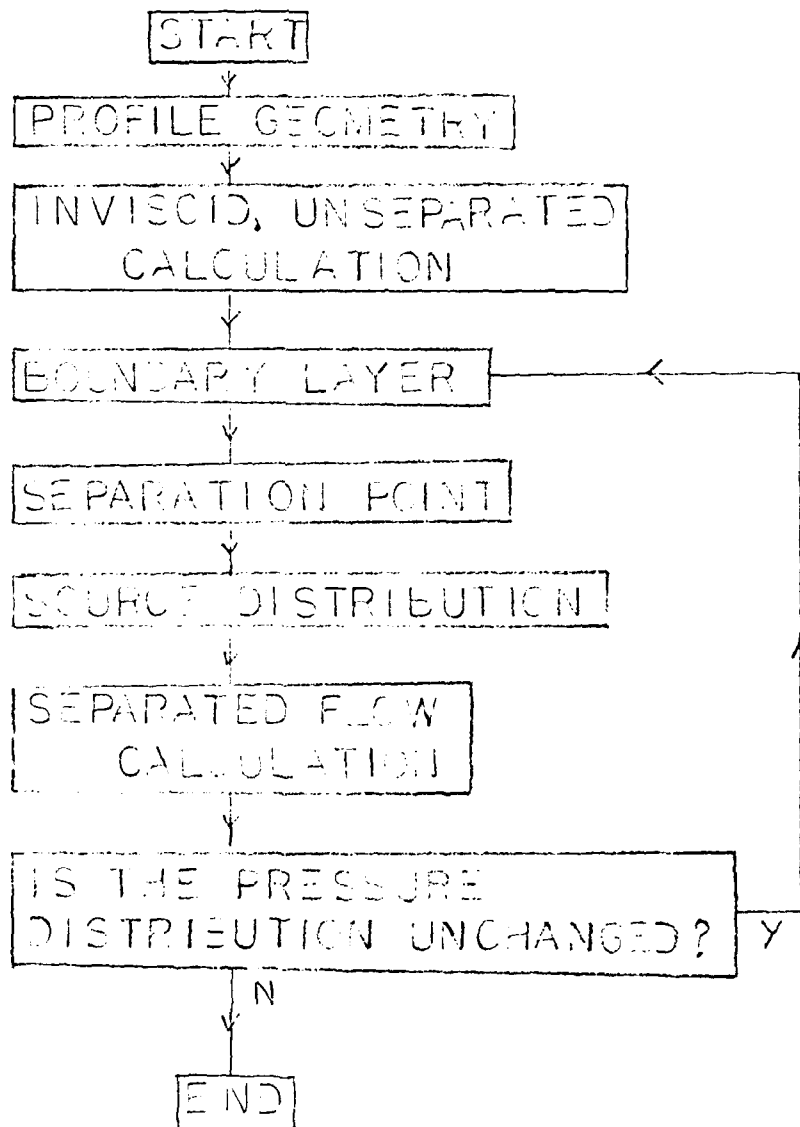


Fig. 4. The Basic Computational Procedure

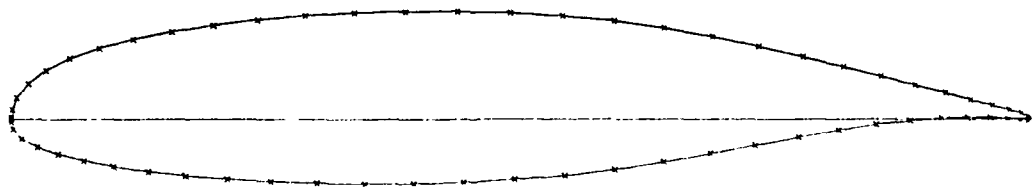
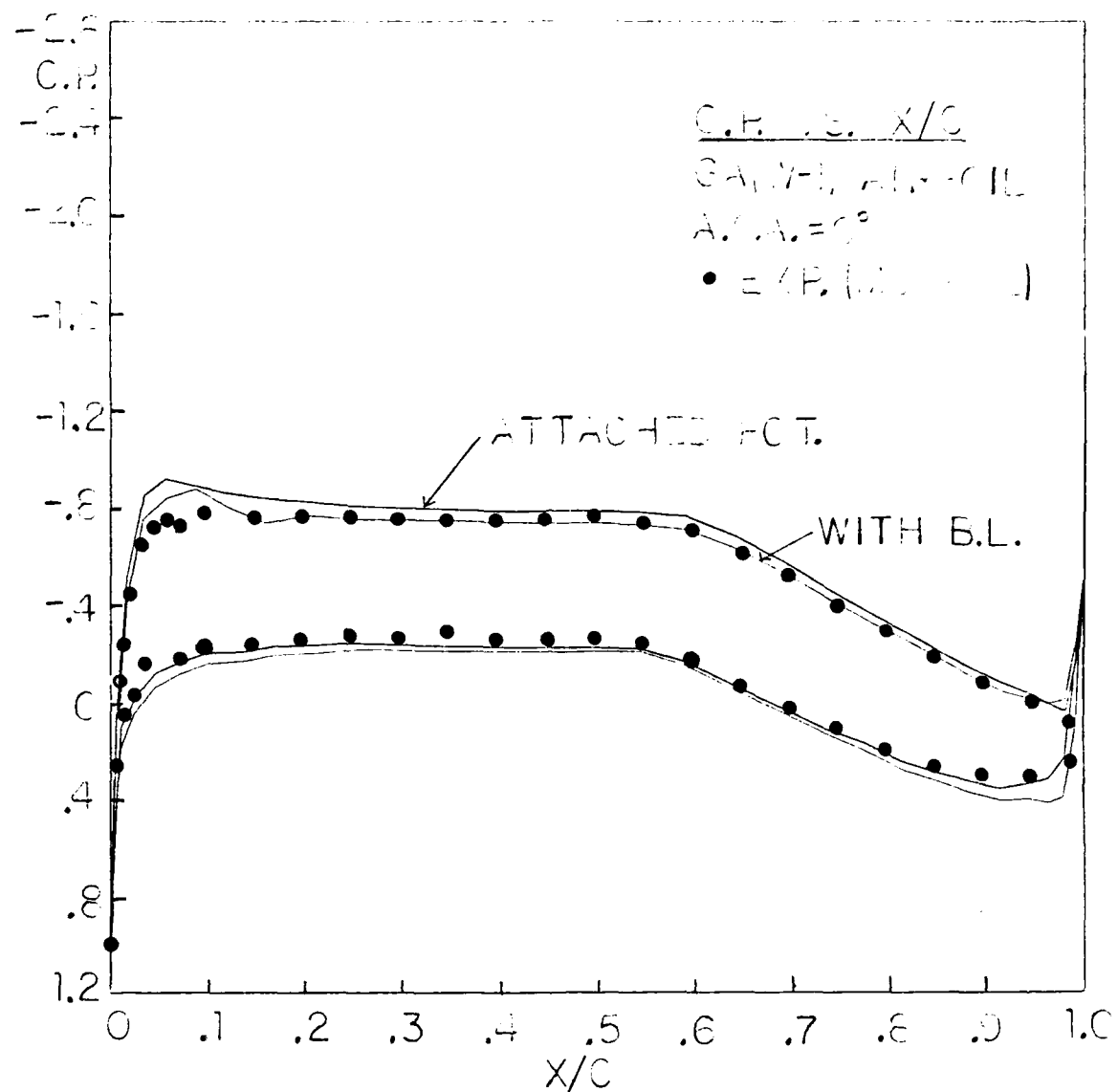


Fig. 5, Pressure Coefficient for GA(W-1)

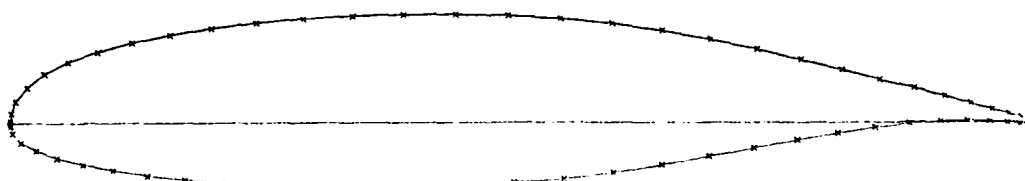
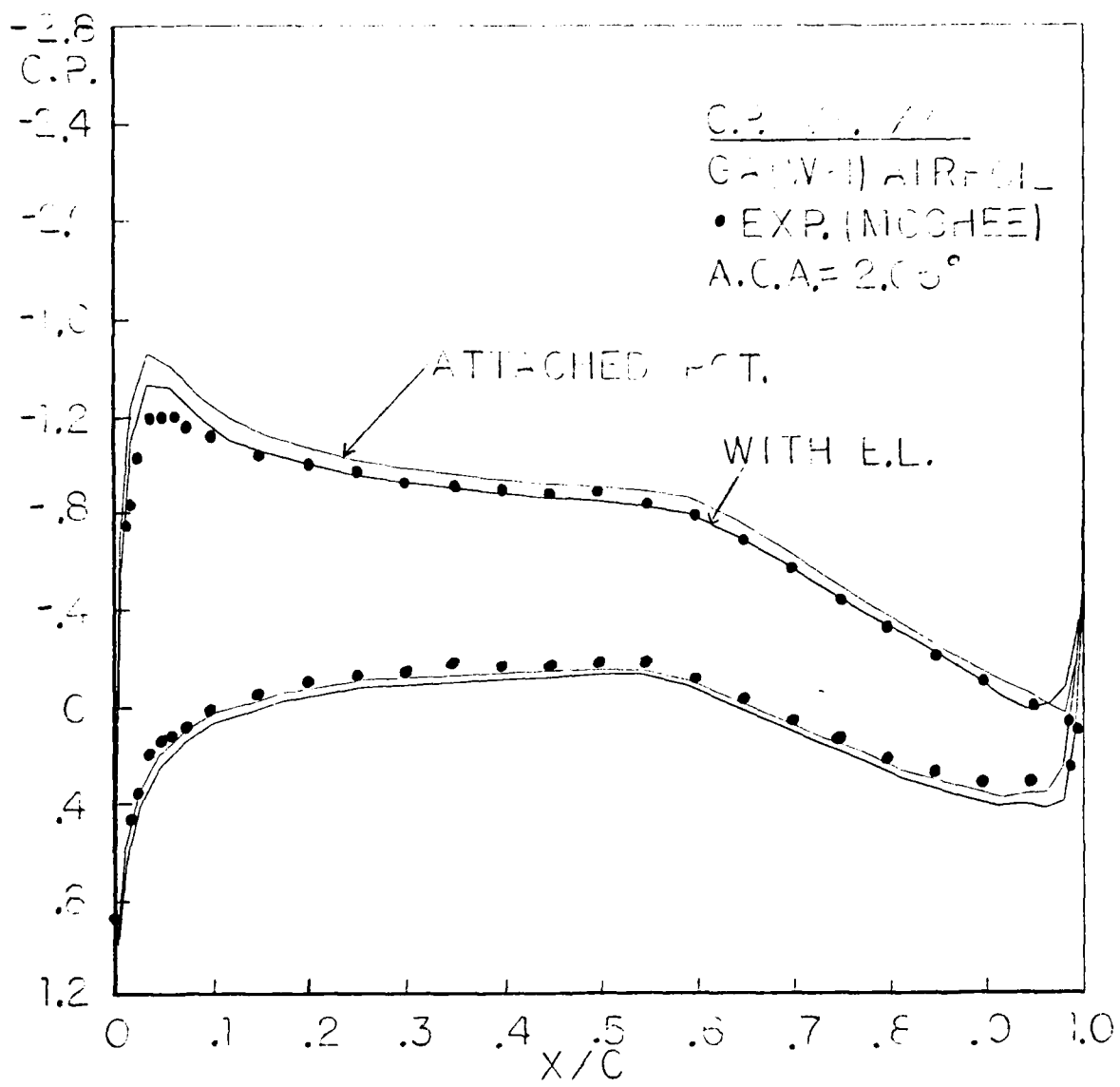


Fig. 6. Pressure Coefficient for GA(W-1)

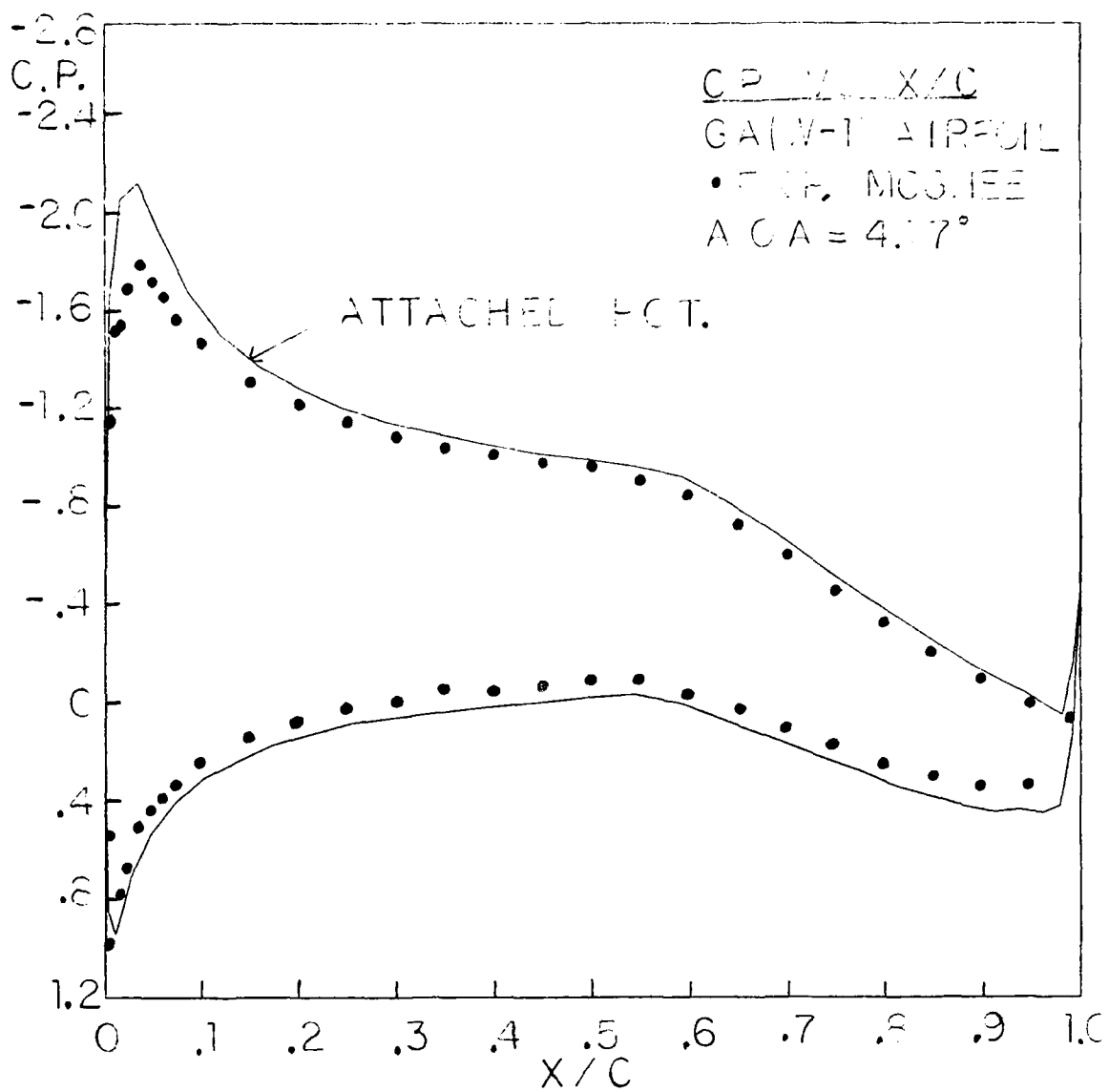


Fig. 7. Pressure Coefficient for GA(W-1)

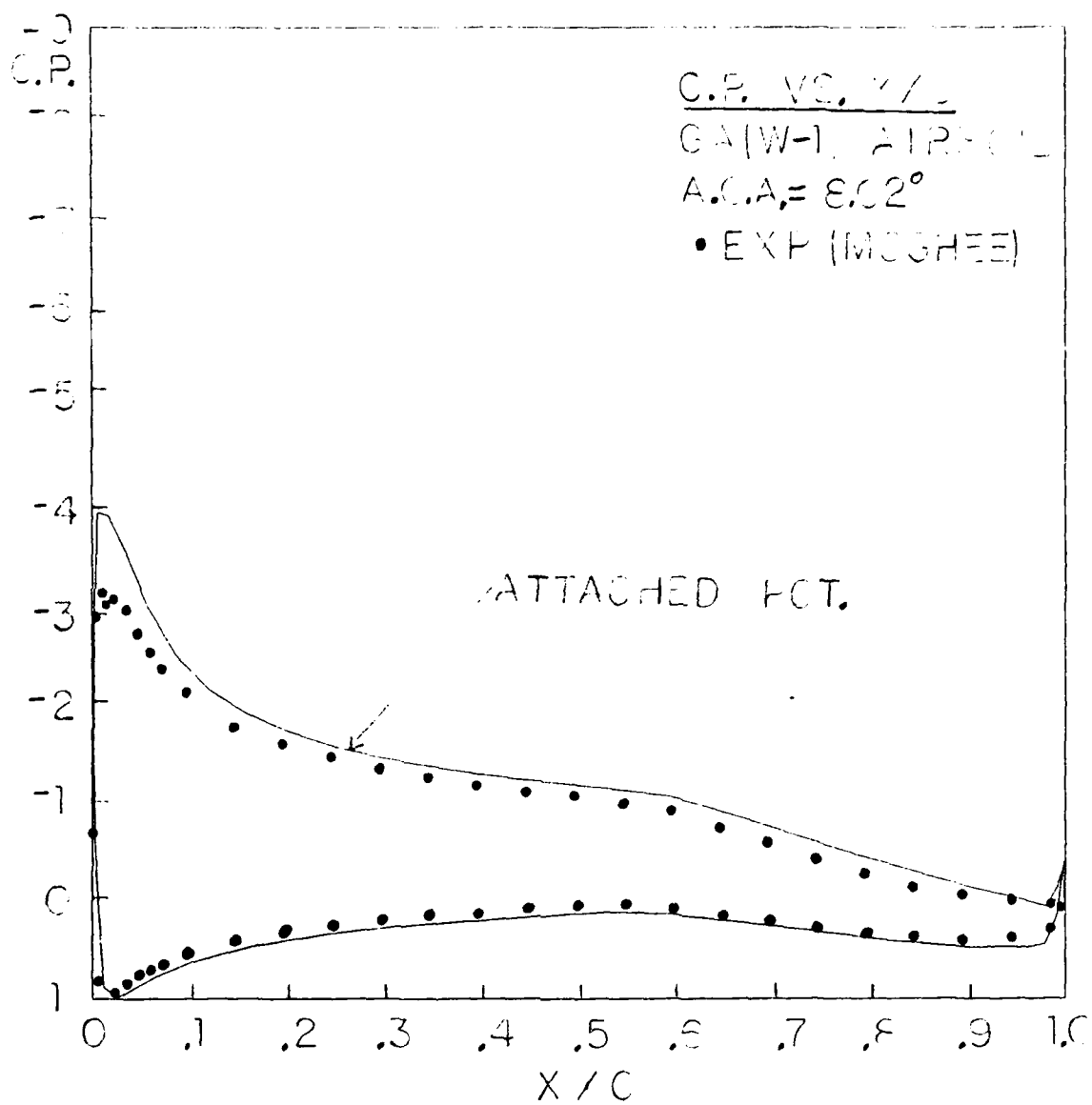


Fig. 8. Pressure Coefficient for GA(W-1)

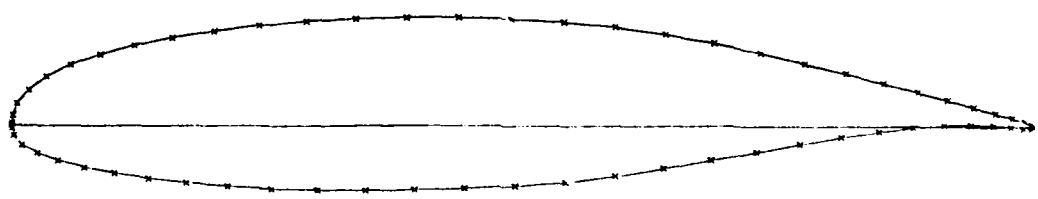
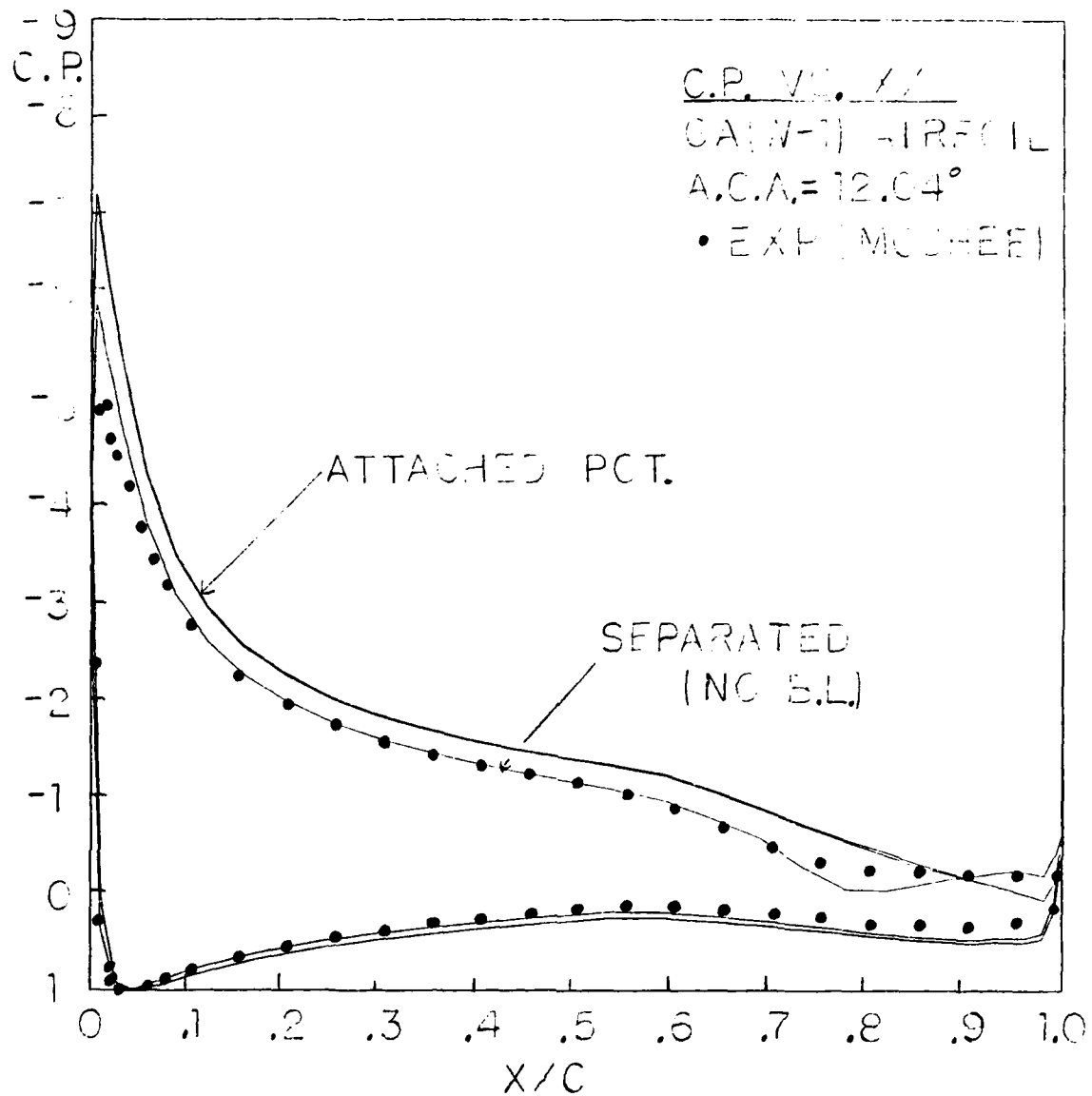


Fig. 9. Pressure Coefficient for GA(W-1)

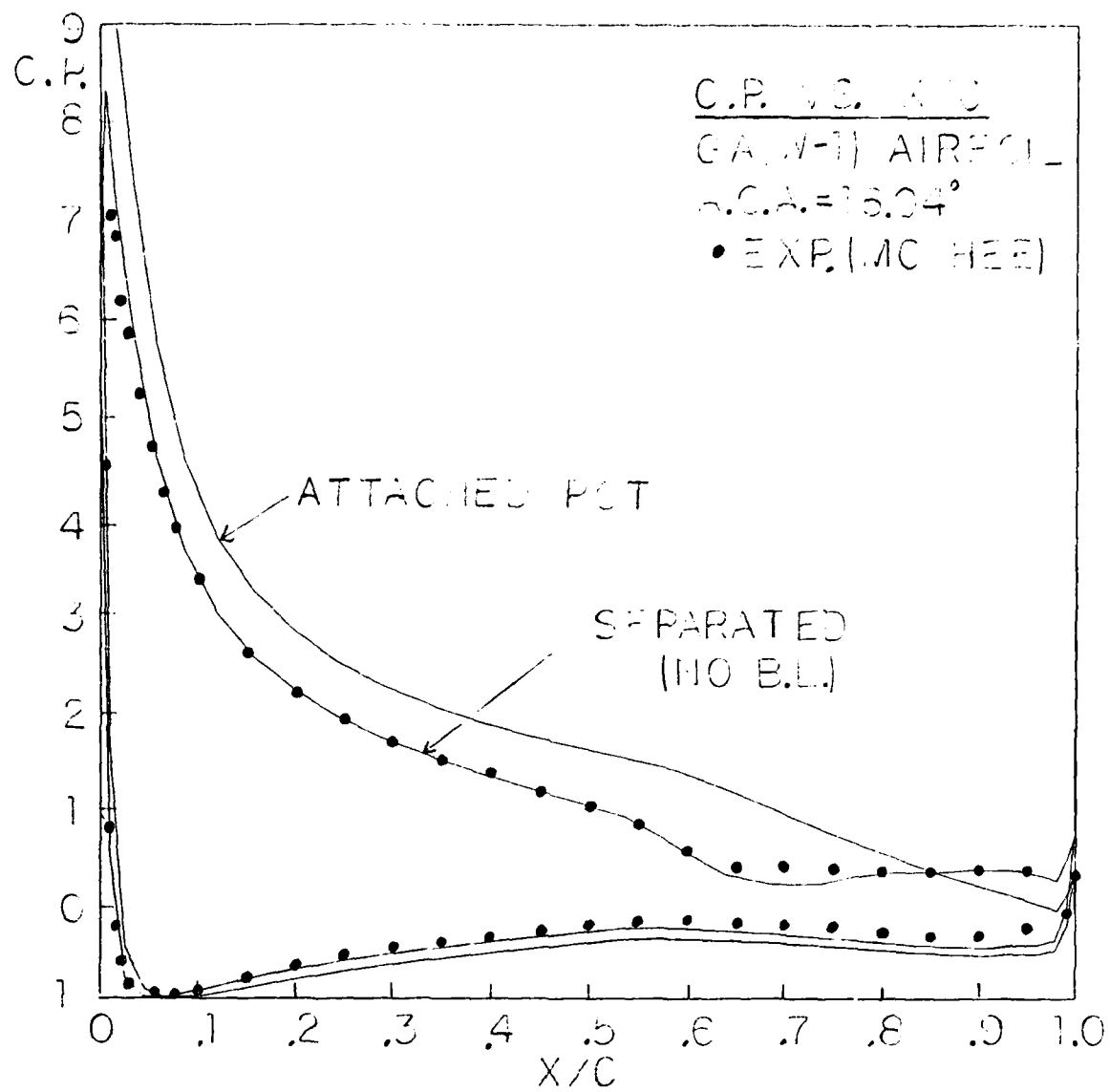


Fig. 10. Pressure coefficient for GA(W-1)

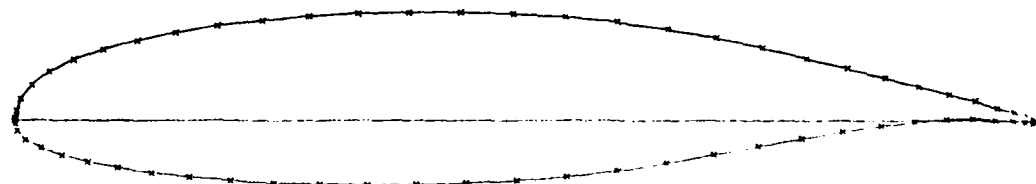
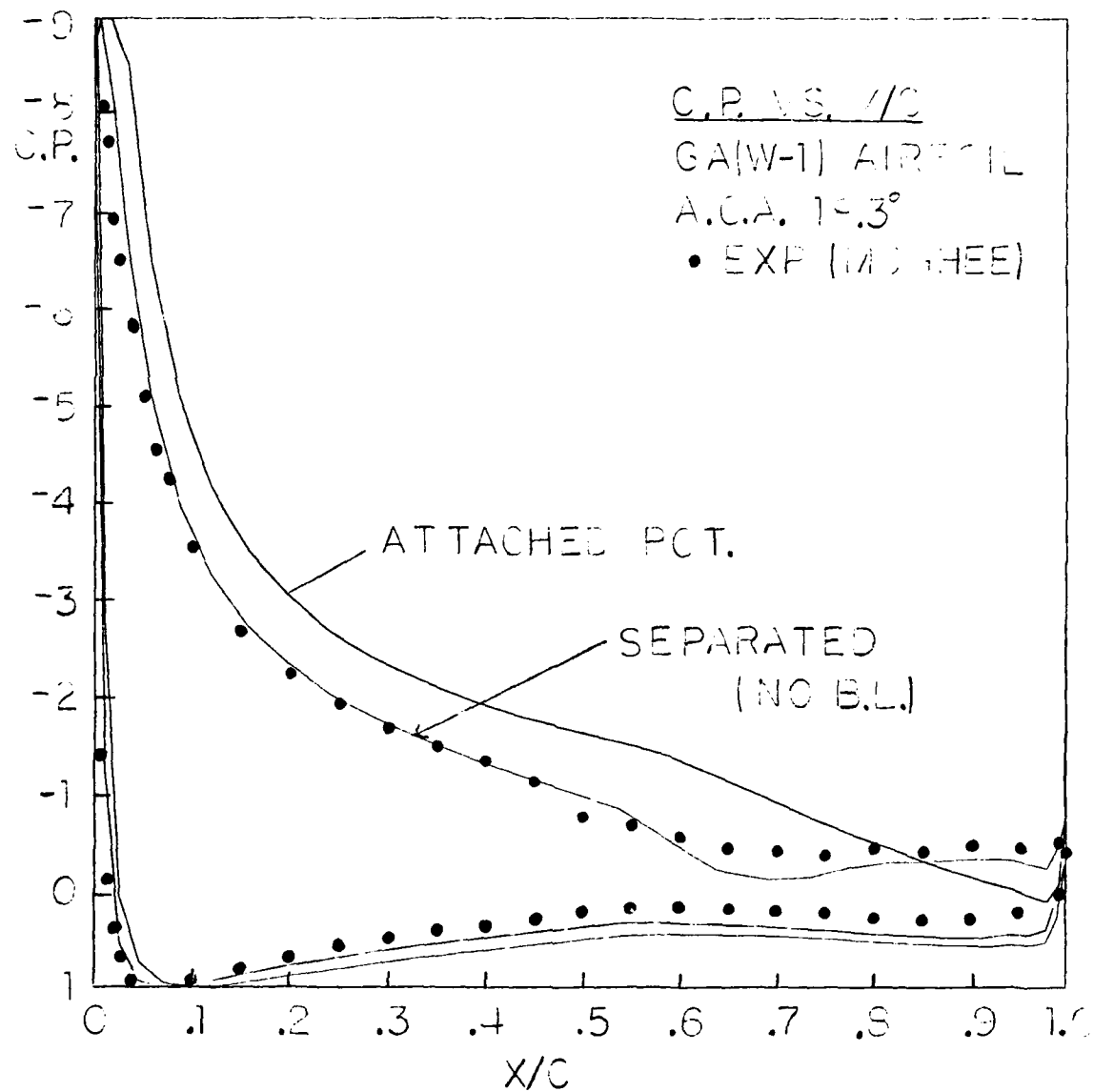


Fig. 11. Pressure Coefficient for GA(W-1)

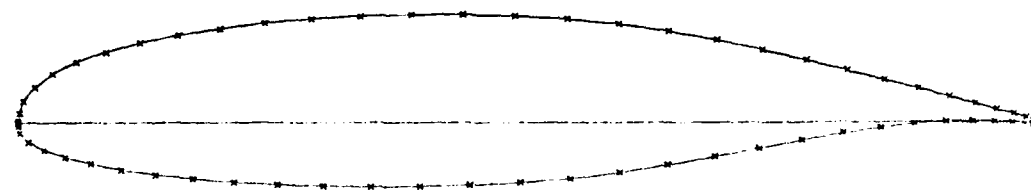
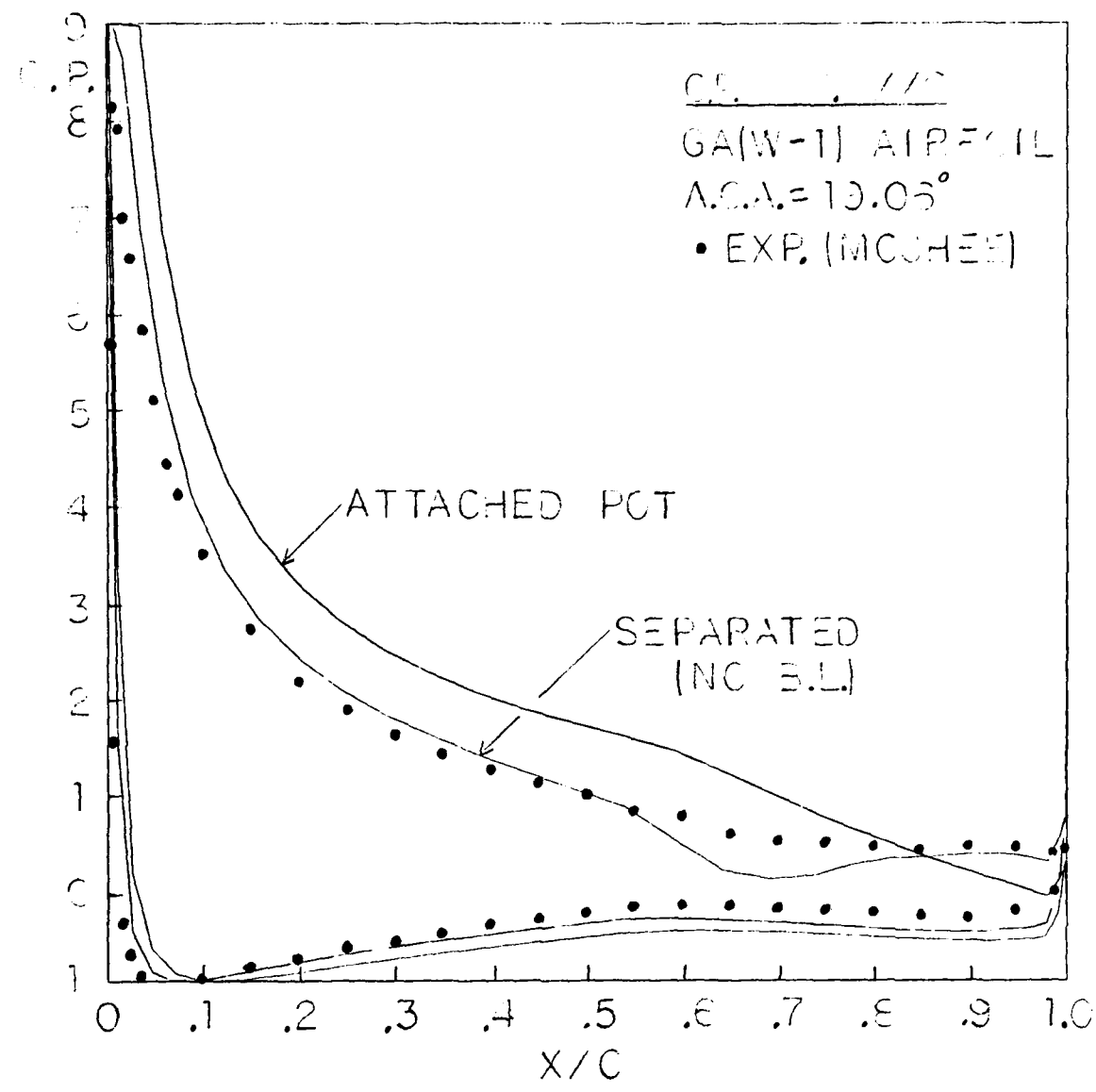


Fig. 12. Pressure Coefficient for GA(W-1)

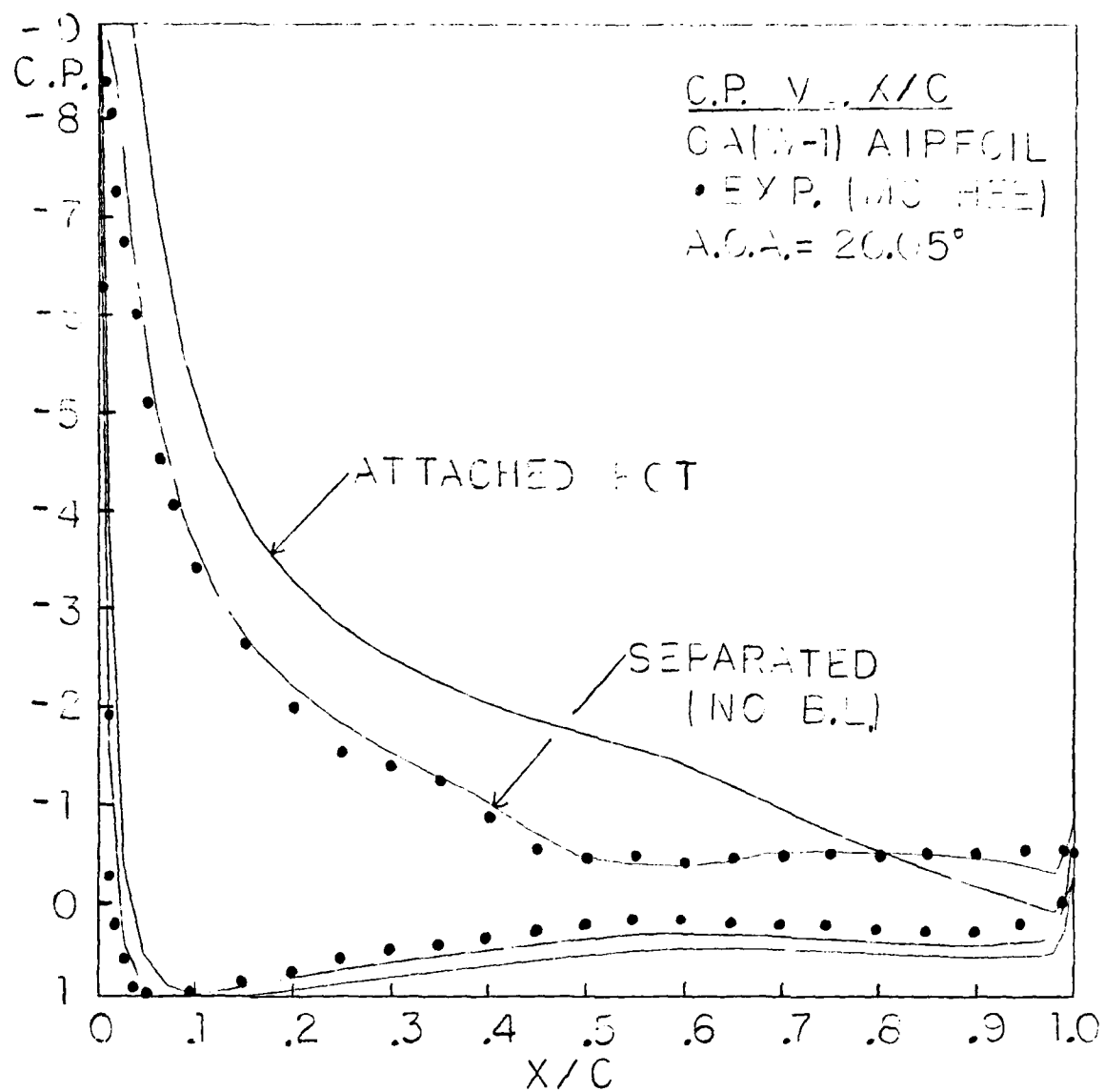


Fig. 13. Pressure Coefficient for GA(W-1)

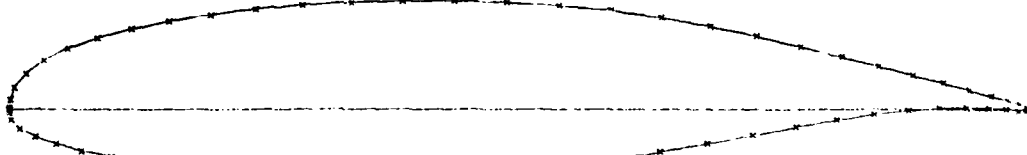
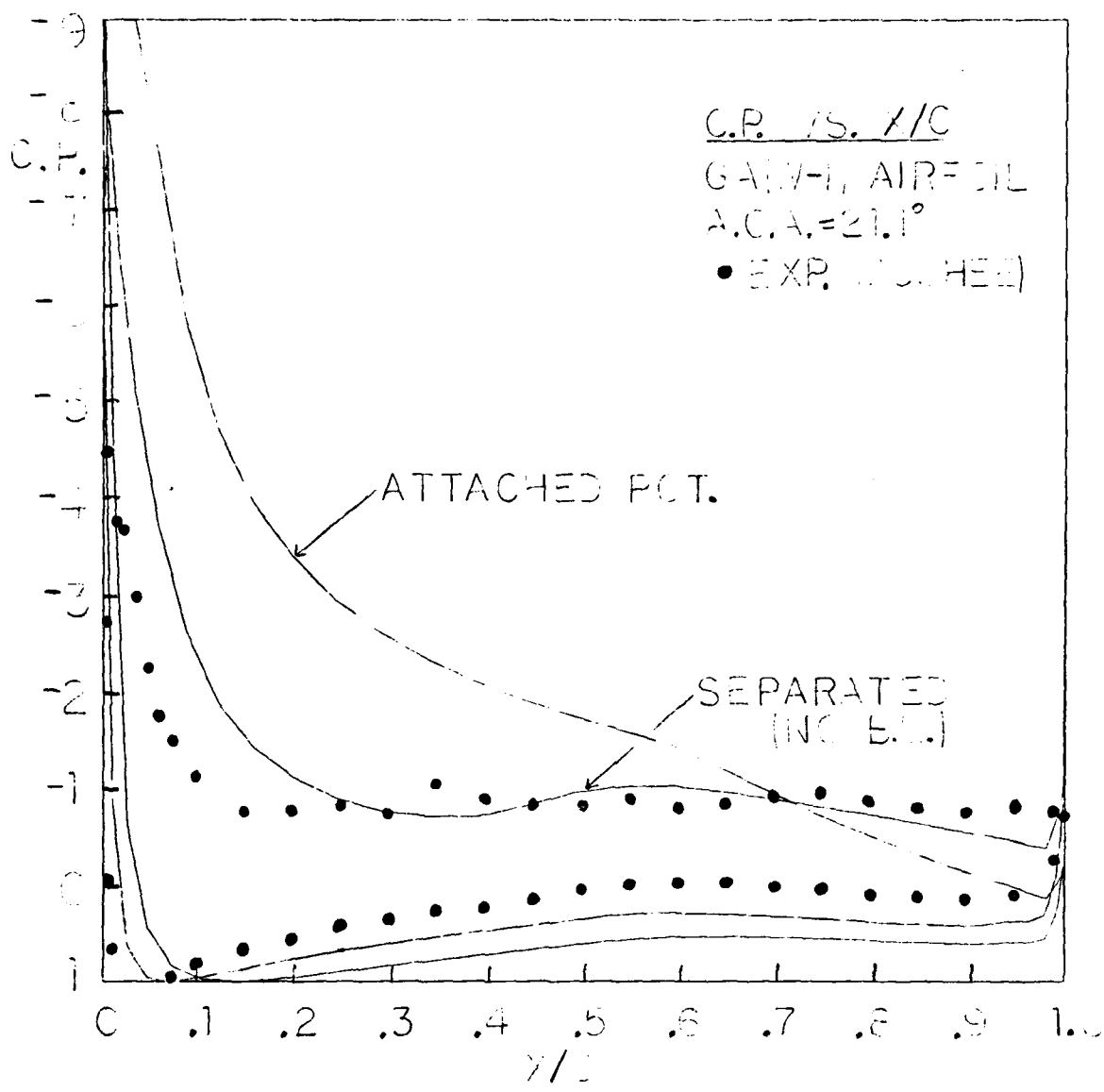


Fig. 14. Pressure Coefficient for GA(W-1)

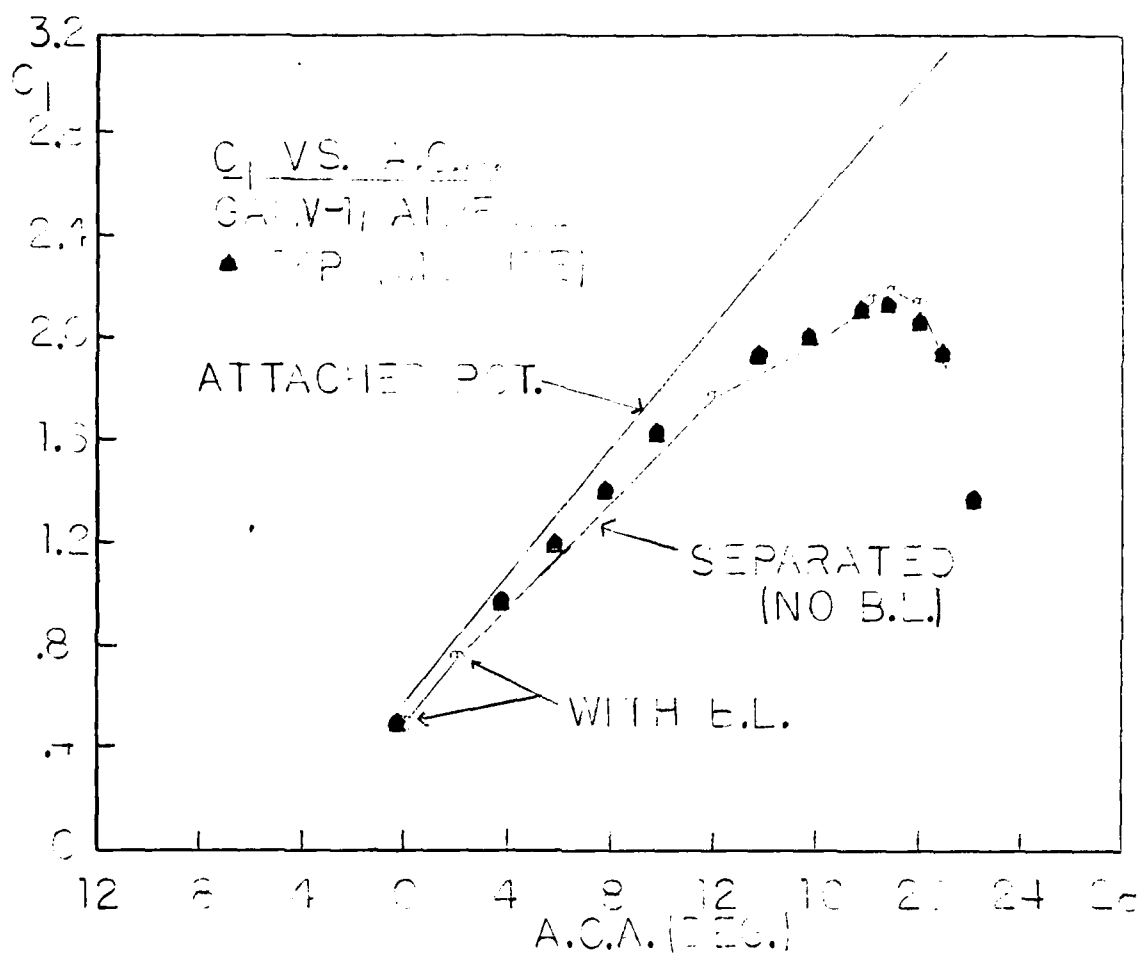


Fig. 15. Lift Coefficient for GA(W-1)

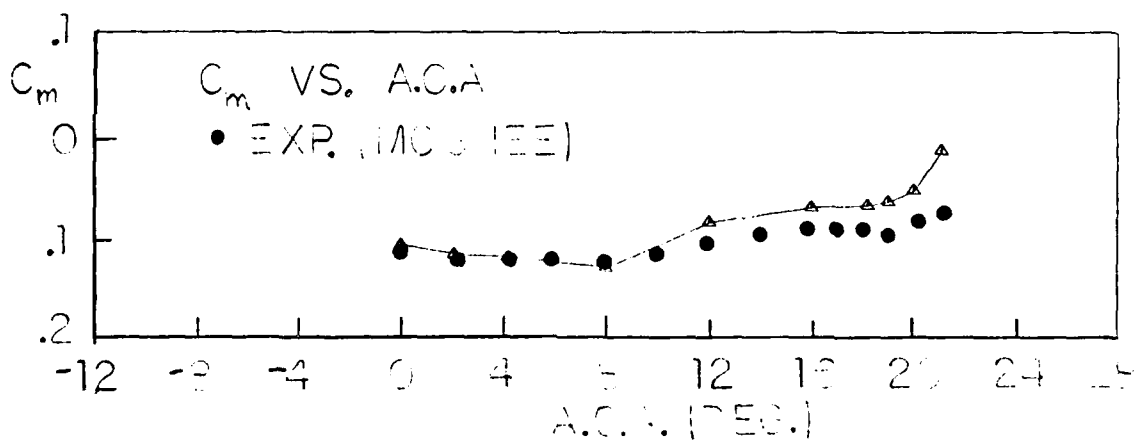


Fig. 16. Pitching Moment Coefficient for GA(W-1)

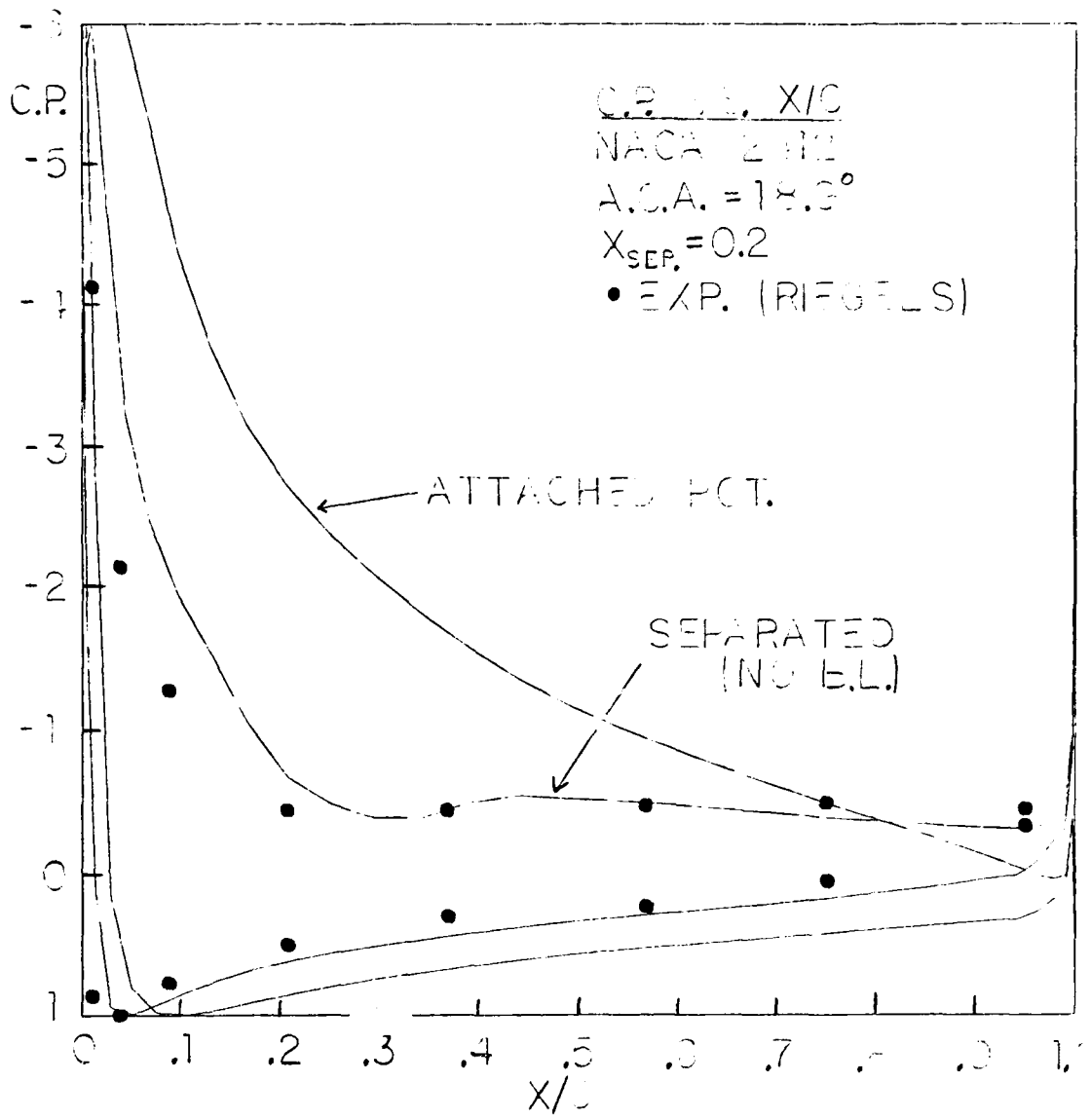


Fig. 17. Pressure Coefficient for NACA 2412

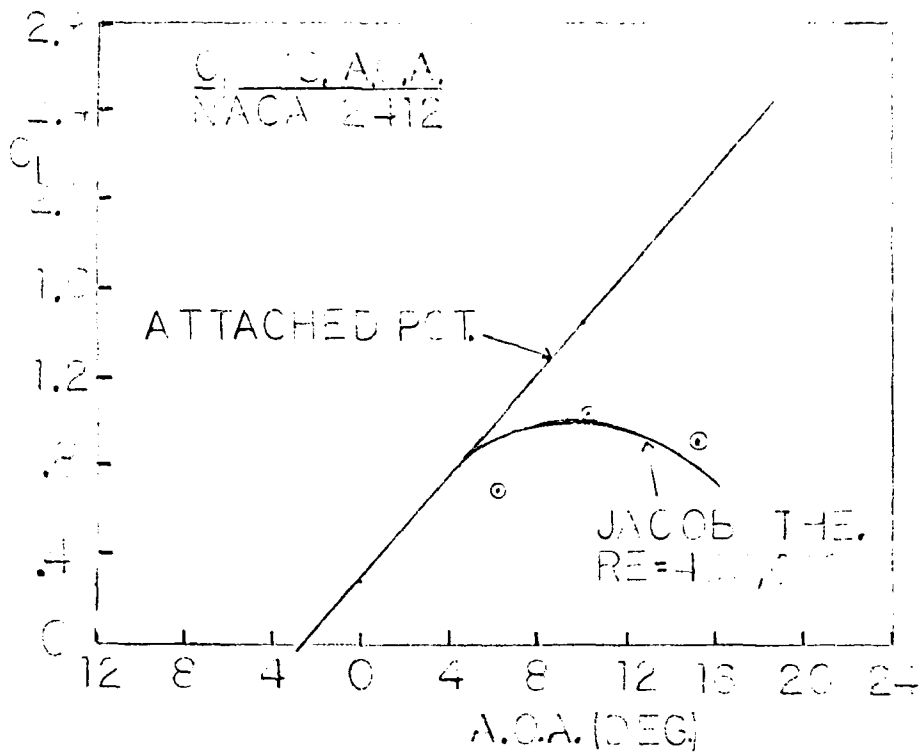


Fig. 18. Lift Coefficient for NACA 2412

END 5-83